POLITECNICO DI TORINO

Master of Science in Energy and Nuclear Engineering

Application of Pinch-Analysis to the charging and discharging processes of Thermo-Chemical Energy Storage for Concentrated Solar Power plants

Supervisors

Prof. Vittorio Verda

Prof. Elisa Guelpa

Dott. Umberto Tesio

Candidate

Giulia Novero

March 2020

SUMMARY

Introduction

The most urgent and decisive challenge of our time is to reduce the impact of climate change on our planet. The main driver of global warming is the increase of carbon dioxide emissions due to the growing anthropization of the environment and the intensive land use. In recent years, mitigation actions against the increase of average surface temperature has concerned the containment of greenhouse gas emissions by promoting a new energy sector model based on renewable energy sources, discouraging the fossil fuels utilization.

According to the International Energy Agency (IEA), the energy transition to be effective will have to lead to the reduction of roughly 45% of the current carbon dioxide emissions by 2040. Nowadays, renewable energies cover about 25% of global electricity supply and the prospect is to double the contribution by 2040. Efficient integration of RES power generation technology is essential for a gradual transition in the energy sector. Storage systems play a fundamental role in the further development of RES in decoupling energy production and demand, since the latter are affected by discontinuity and territorial dispersion.

Among renewable energy technologies, Concentrated Solar Power (CSP) plants have a great potential for integration with Thermal Energy Storage (TES) systems. Over recent years, large scale energy storage applications have been proposed in order to increase the solar energy penetration into the electricity grid. Among the different storage technologies, the Thermo-Chemical Energy Storage (TCES) systems are the most suited for CSP integration. In fact, the TECS is a less mature technology but with a significant higher energy density and potentially capable of decoupling energy production and demand by means of chemical loops.

In this framework, one of the most promising systems for the development of TCSE at large scale is the Calcium Looping (CaL) process, i.e. a chemical loop based on

reversible exothermic reaction of carbonation of CaO with CO_2 to obtain $CaCO_3$ and the reverse endothermic reaction of calcination.

Calcium Looping (CaL) technology integrated in a CSP tower plant has been recently investigated in the European project SOCRATCES to demonstrate its technological, economic and sustainable feasibility. In fact, SOCRATCES global objective is basically to develop a prototype of CSP-CaL integration plant to overcome the issues of intermittent energy generation in CSP applications. The strengths of SOCRATCES project are the use of cheap, abundant and non-toxic materials (CaO) as well as mature technologies typically used in industry, such as fluidized bed reactor, cyclones or gas-solid heat exchangers.

In this project several plant layouts are explored in order to improve the performance of the CaL-CSP integration, focusing on the opportunities for heat recovery. Firstly, the main characteristics of the components used in the CaL-CSP integration and the power cycle adopted are presented. Afterwards, the design of the heat exchanger network capable of fostering the heat recovery is discussed. Given the time dependency of the charging and discharging phases of the thermochemical storage system, the Pinch-Analysis for batch-processes was carried out in order to create a feasible heat exchangers configuration that allows the correct operation of the integrated CaL-CSP system. The optimized CaL-CSP integration layout as well as showing better characteristics from the heat recovery point of view, allows to reduce the investment costs of the heat exchangers network.

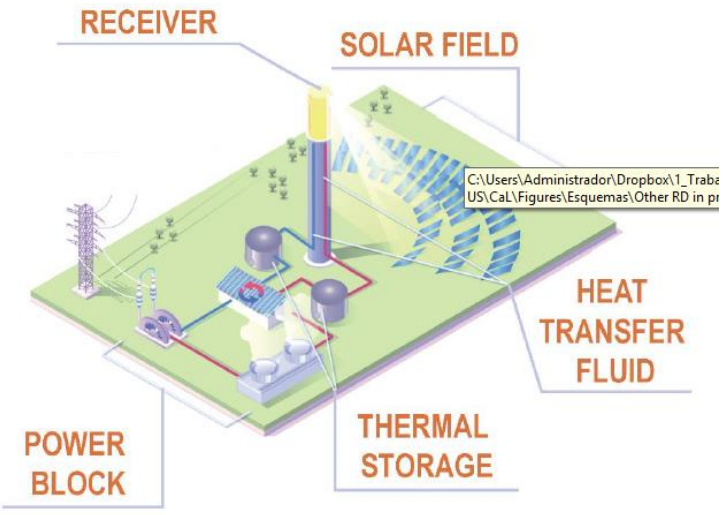

Figure 1. SOCRATCES project layout for CaL-CSP integration **(1)**.

Chapter I

Thermal Energy Storage Systems description

As mentioned before, the Thermal Energy Storage systems play a fundamental role in overcoming the issues of intermittent energy generation in CSP applications..

In fact, a brief explanation of the general aspects of the thermal energy storage is provided to better understand the following discussion.

1.1 General aspects of thermal energy storage

Energy storage is a crucial point for a short-term deeper penetration of renewable energy sources in order to correct the existing mismatch between the discontinuous solar energy supply and the continuous electricity consumption (2).

However, the forms in which the energy can be stored are basically potential, kinetic, electrical and thermal energy form. A CSP plant is able to collect large amount of solar energy through its mirror devices, therefore the most suitable storage system is the Thermal Energy Storage (TSE).

The TES technologies are divided into three storage mechanisms:

- Sensible heat storage
- Latent heat storage
- Thermochemical heat storage

Sensible heat storage system is the most mature and commercial of the three and widely used both at low and high temperature for civil and industrial applications or in solar power plants. This technology is based on the absorption and the subsequent release of heat through a temperature change of a solid or liquid storage medium without either a phase change or a chemical reaction occurring (3). The sensible heat stored $Q[J]$ depends on the temperature variation and can be expressed as:

$$Q = m \cdot \bar{c_p} \cdot \Delta T$$

where $m\,[kg]$ is the mass of the medium, $\bar{c_p}[\frac{J}{kgK}]$ is the average specific heat and $\Delta T\,[K]$ is the temperature variation. Therefore, adequate performances are guaranteed by a proper insulation of the storage installation to reduce thermal losses and by the appropriate choice of the storage materials, such as molten salts, mineral oils and ceramic materials.

Latent heat storage systems exploit the latent heat associated with the phase change in specific materials. In particular, during the charging step, solar energy can be used as heat source that initiates a phase change of the storage medium. Then, the heat is stored in the medium, which is into its new phase, at the charging step temperature. During the discharging step when energy is released, the medium phase changes into the first state. The heat stored $Q[J]$ can be expressed as:

$$Q = m \cdot \lambda$$

where $\lambda\,[\frac{J}{kg}]$ is the latent heat of the material. Phase change materials (PCM) allow attaining higher storage capacities as compared to sensible heat storage. Since the phase change temperature must be sufficiently high, the latent storage systems are also affected by thermal losses.

Thermochemical energy storage (TCES) systems consist of using the heat obtained from an external source such as CSP to drive an endothermic chemical reaction. In general the reaction involved in the thermochemical heat storage system are reversible ones:

$$A + \Delta H_R \leftrightarrow B + C$$

Heat is stored during the endothermic reaction step and released during the exothermic one. The thermochemical heat stored is connected to the reaction enthalpy ΔH_R . During the charging mode, thermal energy is used to dissociate a chemical reactant (A) into products (B) and (C). During the discharge mode, the products of the endothermic reaction (B and C) are mixed together and react to form the initial reactant (A). The products of both reactions can be stored either at ambient temperature or at working

temperature (2). The thermal energy stored in thermochemical material can be expressed as:

$$Q = n_A \cdot \Delta H_R$$

where $n_A[mol]$ is the number of moles of the reactant A and $\Delta H_R[\frac{kWh}{mol}]$ is the reaction enthalpy. The simplified scheme of a TCES is presented in Fig.2.

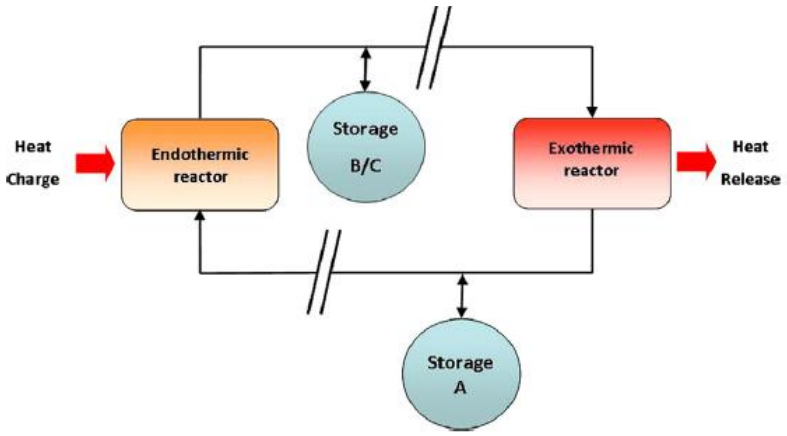

Figure 2. Simplified scheme of a TES system based on chemical reaction **(2)**.

The main advantages of TCES as compared to TES are considerably higher energy density as well as the possibility of storing energy in the long-term or transport it without significant losses. A short summary is reported in Table.1.

	Sensible heat storage	**Latent heat storage**	**Thermochemical storage**
Energy density			
Volumetric density	Small ~ 50 kWh m^{-3} of material	Medium ~ 100 kWh m^{-3} of material	High ~ 500 kWh m^{-3} of material
Gravimetric density	Small ~ 0.02-0.03 kWh m^{-3} of material	Medium ~ 0.05-0.1 kWh m^{-3} of material	High ~ 0.5-1 kWh m^{-3} of material
Storage temperature	Charging step temperature	Charging step temperature	Ambient temperature
Storage period	Limited (thermal losses)	Limited (thermal losses)	Theoretically unlimited
Transport	Small distance	Small distance	Distance theoretically unlimited
Maturity	Industrial scale	Pilot scale	Laboratory scale
Technology	Simple	Medium	Complex

Table 1.1 Characteristic and comparison of the TES systems **(2)**.

1.2 Calcium Looping

Among the storage technologies illustrated above, the thermochemical storage has been chosen for SOCRATCES project. Several reversible reactions have been analysed as TCES, mainly based on carbonates, hydroxides, metal redox, etc. The thermochemical storage system adopted in the SOCRATCES project is based on the Calcium Looping (CaL) process. In past years, CaL technology was extensively studied as a post-combustion CO_2 sequestration system or for limestone production, but recently it has been investigated as a TCES systems for central tower CSP plants integration.

Calcium Looping (CaL) process relies upon calcination-carbonation reaction of $CaCO_3$/CaO. In the first step, concentrated solar power is used to carry out the endothermic calcination reaction of $CaCO_3$ (calcium carbonate or limestone) releasing CO_2 and CaO (calcium oxide or lime) as products that are stored separately.

$$CaCO_{3(s)} + \Delta H_r^0 \rightarrow CaO_{(s)} + CO_{2(g)} \quad with\ \Delta H_r^0 = 178.4 \frac{kJ}{mol}$$

When energy is needed, the stored products are brought together to carry out the exothermic carbonation reaction which releases the stored energy.

$$CaO_{(s)} + CO_{2(g)} \rightarrow CaCO_{3(s)} + \Delta H_r^0 \quad with\ \Delta H_r^0 = -178.4 \frac{kJ}{mol}$$

The CaO and the $CaCO_3$ chemically react in the solid state after being reduce into powders to enhance the rate of reaction and facilitate their transport.

Furthermore, the different operating conditions of the TCES systems were analysed considering the equilibrium states of the reversible reactions, that are defined by thermodynamic parameters such as pressure and temperature. In particular, studies performed on the reversible carbonation reaction between CaO and CO_2 have provided an equilibrium equation expressing the partial pressure of CO_2 in equilibrium condition as a function of temperature (3):

$$p_{CO2,eq} = 4.137 \cdot 10^7 \exp\left(-\frac{20474}{T_{eq}}\right)$$

where p_{eq} is expressed in [bar], while T_{eq} is in [K] and it is shown in Fig.3. The partial pressure axis is in logarithmic scale. Consistently with the Le Chatelier's chemical

equilibrium principle, the reaction of calcination takes place at high temperature and low CO_2 partial pressure values, while the carbonation reaction is favored by high CO_2 partial pressure and low temperature values (4). Moreover, the atmospheric pressure value is indicated to examine the corresponding equilibrium temperature. The reaction turning temperature is defined as the temperature at which the reaction occurs spontaneously. As shown in the figure below, when CO_2 partial pressure is equal to atmospheric pressure, the equilibrium temperature is approximately 895°C (5). Therefore, the endothermic calcination reaction occurs in a spontaneous way when the turning temperature is reached; on the contrary, the exothermic carbonation reaction requires lower temperatures for the release of thermal energy.

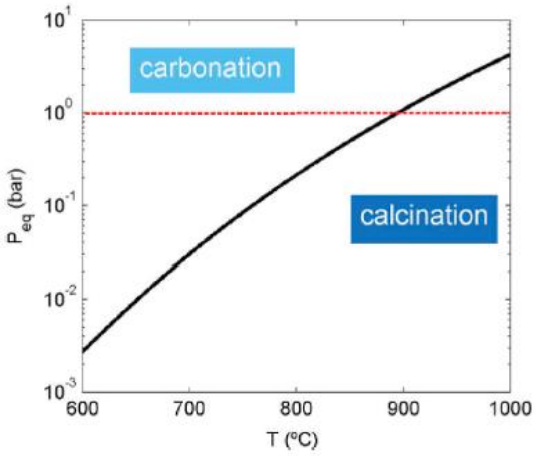

Figure 3. CO_2 partial pressure as a function of temperature at thermodynamic equilibrium for the calcination/carbonation reaction of $CaCO_3$/CaO. At atmospheric pressure is indicated by dashed line **(5)**.

After analysing the thermodynamic characteristics of the CaL reactions, it is necessary to discuss about the physic-chemical aspects related to the materials used in the CaL process, which highly affect the overall efficiency of the TCES system (5).

In the Calcium Looping process, the CaO is subjected to repeated cycle of carbonation/calcination and its reactivity is negatively influenced by the increasing of number of cycles.

In Thermo-Gravimetric Analysis (TGA) experiments, the sorbent reactivity X is defined as the ratio between the reacted amount of calcium oxide at the end of carbonation stage and its stoichiometric quantity (3):

$$X = \frac{mol\ CaO_{reacted}}{mol\ CaO_{stoichiometric}}$$

Moreover, different cycling experiments have been performed on a $CaCO_3$ sample in order to investigate the mass variation during carbonation/calcination cycles (3). In the y-axis is reported the percentage weight of the amount of $CaCO_3$ in the solid phase of reactants and products. During calcination the sample weight drops from its initial value, as calcium carbonate is converted in CaO and gaseous CO_2. Then, the temperature is switched so that the carbonation occurs and the sample mass increases without ever returning to initial value, therefore indicating a loss of reactivity (3) (4). At this point, the sample is again subjected to the calcination process and so on. As shown in Fig.4, after carbonation process, the sample weight decreases up to an asymptotic residual value as the number of cycles increases. On the contrary, after calcination, the sample mass remains almost the same.

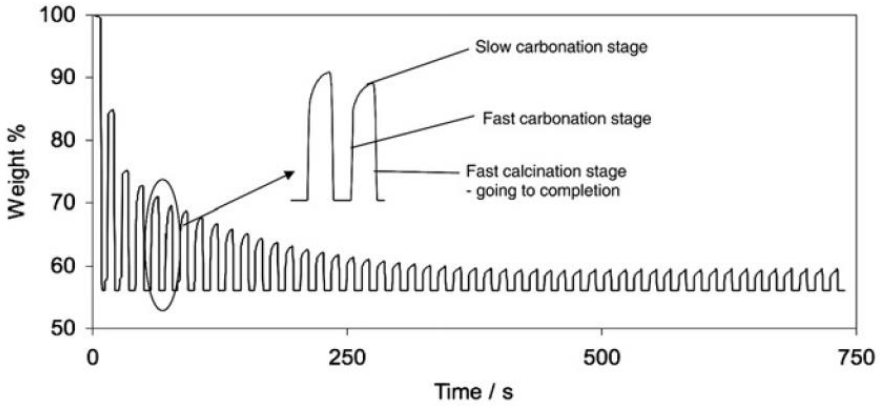

Figure 4. Mass drop in repeated carbonation/calcination cycles (3).

The physical explanation of the material reactivity drop in Calcium Looping lies mainly in two complementary phenomena:

- Pore-plugging de-activation mechanism
- Sintering de-activation mechanism.

The carbonation reaction kinetics consists of two consecutive and differentiated stages. The first phase is rapid, chemically controlled and determined by the kinetics of the reactants (CaO and CO_2). After that, the fast carbonation stage ends with the formation of a calcium carbonate ($CaCO_3$) layer around the particle of the sorbent (CaO). When the thickness of the $CaCO_3$ layer reaches a critical value, both the active surface and the number of pores of CaO grains are reduced (4). Consequently the CaO particles are no longer able to react directly with the CO_2 and the carbonation is significantly slowed

down, because the process relies entirely on the solid diffusion phenomena of CO_3^{2-} and O^{2-} mobile ions (3; 5). The reaction rate changes between fast/slow carbonation stages determine a reduction of reactivity because a consistent number of pores do not re-open in the calcination phase (3).

The second de-activation mechanism is sintering, which is a temperature-driven phenomenon responsible for the growth of small pore and grains of the CaO particles in CO_2-rich environment that accelerates the loss of reactivity (3). Sintering is promoted by high temperatures, i.e. half of melting temperature (for CaO is approximately 533°C) and by high CO_2 partial pressure in the calcination environment (3).

As already mentioned, the CaL process has been firstly studied as a post-combustion CO_2 capture system. Such applications necessarily involve carbonation under low CO_2 partial pressure, which is imposed by the low CO_2 concentration in the flue gas exiting the power plant, while calcination requires both high CO_2 partial pressure and temperature (around 950°C) (5). After a large number of cycles CaO conversion converges asymptotically towards a residual value of just about X=0.07–0.08 for limestone derived CaO and carbonation/calcination residence time about 5 min (5) (6). On the other hand, the specific conditions for an efficient integration of CaL process into CSP plants involve carbonation both at high CO_2 partial pressure and temperature. Experimental results from TGA tests show the different behaviour of CaO conversion X as a function of carbonation/calcination cycle number N for both CO_2 capture system and CSP energy storage (Fig.5). The obtained residual CaO conversion for CaL-CSP integration is around X=0.53, considerably larger than the value for CO_2 capture conditions (6).

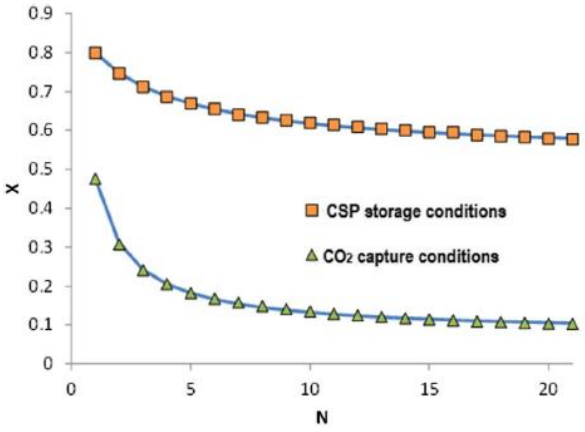

Figure 5. Multi-cycle conversion of limestone derived CaO under different CaL conditions **(6)**.

Chapter II

Technological aspects for the Integration of CSP and Thermochemical Energy Storage

The SOCRATCES project aims essentially to demonstrate the feasibility of CaL-CSP plant integration by exploiting different technologically mature components in terms of solar calcination, heat transfer, material transport and solid gas separation (6) (1).

A conceptual scheme of the CaL-CSP integration for thermochemical energy storage is provided in Fig. 6. The calcination reaction occurs in the receiver of CSP plant central tower, since the solar concentrator is capable of providing high thermal energy for the endothermic process. On the other side, the exothermic carbonation process releases high temperature heat used in the power cycle, both for direct and indirect configuration. Therefore, the processes are divided into two physically independent blocks: the calciner side and the carbonator side in order to separate the heat storage and the power generation phase (5).

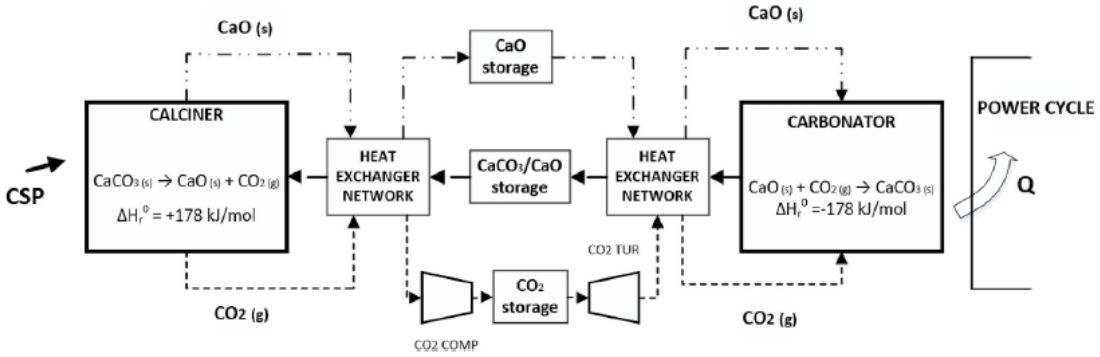

Figure 6. Conceptual diagram of Calcium Looping- CSP plant integration **(5)**.

As shown in Fig. 6, heat storage occurs in the solar calciner where the concentrated solar radiation leads to the $CaCO_3$ calcination. Then, the CO_2 exiting the calciner is sent to a storage tank after being cooled and compressed, while the CaO solid stream is transported to its own storage system once the ambient conditions are reached (6). The

energy release phase takes place in the carbonator side where the high temperature heat produced in carbonation reaction is released to a power cycle (7).

In this section, the main features of the components integrated in the CaL-CSP system are described, since they affects both aspect of scaling-up and solar-to-electricity efficiency of modelled installation (5).

2.1 Solar Calciner

Among the receiver technologies for CSP application, a solar tower configuration with a direct adsorption receiver is the most suitable option for CaL-CSP integration. The solar radiation reflected by the heliostats field is concentrated on the central receiver allowing it to reach the high temperatures required by calcination process (5). The Fig.6 shows a diagram of the designed installation where the circular irradiated reactor is crossed by the falling particles of $CaCO_3$. However, the calcination temperature must be kept as low as possible to limit the effects of CaO de-activation mechanisms. According to chemical equilibrium conditions, low reaction temperatures require low CO_2 partial pressures to complete the calcination process in short residence time (7). During the calcination process a continuous CO_2 flow is generated inside the calciner, causing an increase in the partial pressure of the gas and consequently an increase in reaction temperature even above 900°C (8). Since the solar calciner operates at ambient pressures, the CO_2 partial pressure must be returned to the atmospheric value by adding another "diluent" gas into the calcination environment. After having analysed different diluent gases, steam was the most advantageous one in terms of availability and management of the reactor functions. In fact, by introducing superheated steam in the calcination atmosphere, the reaction temperature can be reduced to 700-750°C. The use of steam is beneficial both to accelerate the reaction kinetics and to improve the CaO reactivity limiting the sintering effects.

In recent years, several calciner systems have been considered for CaL-CSP integration design among those already patented. Initially a pilot-scale system of a Catalytic Flash Calcination (CFC) technology was developed by Calix Limited company for the carbon capture and processing industry based on the use of magnesium carbonate as raw material (3) (8). A graphical representation of the CFC reactor for CCS application is provided in Fig. 7. Subsequently, the SOCRATCES project dealt with the re-design of a limestone CFC suitable for a CSP plant integration (8). In particular, the Catalytic Flash

Calcination technology under investigation is based on a entrained flow reactor enhanced by superheated steam flow. The calciner technology allows the solid $CaCO_3$ powder to be fluidized in a steam bed which acts as a reaction catalyst, heat transfer medium, solid matter carrier and finally reduces the reaction temperature (3) (4). The complete decomposition of the particles is obtained in short residence times (2 or 3 seconds) when the steam participates in the calcination process (4). About the reaction products, the solid stream is separated by means of a cyclone whereas a condenser is used to separate the steam from pure CO_2 flow (3).

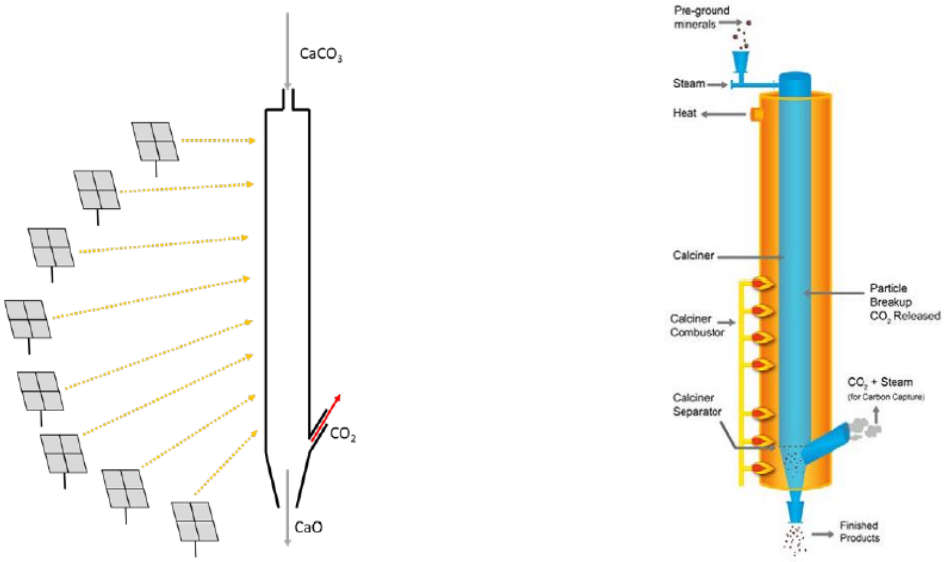

Figure 7 . a) Irradiate tube reactor design in the central solar tower of CSP installation **(8)**. *b) Catalytic Flash Calciner developed by Calix Limited for CCS applications* **(8)**.

The solar receiver thermal efficiency is clearly affected by the heat transfer losses associated with the high temperatures involved in the calcination process. In particular, radiative losses can be limited by reducing the operating temperature of the solar reactor, for instance by adding steam into the calcining environment, the temperature drops to around 750°C compared to the typical 900°C of pure CO_2 calcination. Besides, the convective losses can be mitigated by enhancing the thermal insulation of the solar receiver. Minimizing heat transfer losses as much as possible enables existing, reliable and commercially competitive technologies to be exploited (4).

2.2 Carbonator

The most widespread and technologically mature component adopted in the SOCRATCES project as a carbonator is a Fluidized Bed reactor (FB). As mentioned before, Fluidized Bed reactors have been used in the environmental, chemical and

processing industries and can potentially be exploited in the thermochemical energy storage systems, such as the CaL process (5). Compared to the calciner technology, the FB reactor used as carbonator represents a simpler and more reliable component whose different models have been analysed in past literature (5).

The working principle of the carbonator essentially consists in conveying the solid particles of CaO into the reactor though a pure CO_2 flow that also acts as a fluidizing medium. Homogeneous fluidization in a gas-solid reactor is a critical aspect basically due to the presence of CaO solid particles both as a inlet stream in the carbonator and as an inert compound (5). Fluidization performance improvements are guarantees by the correct particle size of the powdered CaO and also by an excess of inlet CO_2 flow in terms of mass flow rate supplied to the carbonator, which meanwhile allows more efficient control of the reactor temperature (3) (4). As regards the management of the outlet carbonator streams, a cyclone is used to separate the excess of CO_2 from the solid compounds, i.e. the $CaCO_3$ and the CaO not reacted.

As already discussed, the thermodynamic parameters of the carbonation reaction play a fundamental role in determining the reactor functions. Normally, a higher molar fraction of CO_2 is introduced into the carbonator in order to increase the kinetics of both fast and diffusive carbonation due to an higher CO_2 partial pressure. Similar advantages are given by a pressurized carbonator because the increase in the total pressure of the reactor implies the growth of the CO_2 partial when the molar fraction of inlet CO_2 flow is kept constant. Moreover, the TGA tests revealed that the CaO originated by high-pressure carbonation shows a lower reactivity loss in multi-cycle conversion compared to the atmospheric carbonation (3). The reaction rate can be improved until the total pressure of the carbonator reaches 5.3 bar, i.e. the limit value at which the reaction kinetics is no longer affected by the increase of CO_2 partial pressure (3).

Finally, the high temperature thermal energy produced in the carbonator is released in a power cycle, given the exothermicity of the carbonation reaction. The temperature typically varies between 650°C and 1000°C depending on the operating conditions of the reactor and clearly the higher the carbonator temperature, the greater the efficiency of the entire configuration of the plant (4).

2.3 Heat exchangers

As shown in Fig. 6, the CaL-CSP integration scheme includes a heat-exchangers network to improve the overall plant efficiency by exploiting the large temperature differences between inlet and outlet streams in the carbonator, in the calciner and in the storage tanks (5). Based on the fluids involved in heat transfer both for the CaL process and for power production, the heat exchangers configurations that can be used are gas-gas, gas-solid and solid-solid.

A gas-gas heat exchanger is the most technologically and commercially developed type and operates only in a closed configuration, i.e. the gases are maintained separately from one another. In the CaL-CSP application a gas-gas heat exchanger could be adopted not only to cool the high-temperature stream of CO_2 exiting the solar calciner, that must be brought into the desired storage conditions, but also as a regenerator of the CO_2 close-loop for power generation (5).

A gas-solid heat exchanger can work either in an open or closed configuration based respectively on a direct or indirect contact between the two streams. Among the open configuration, the most widespread technology is the axial flow cyclone heat exchanger (3). By means of a feeding tube, the solid particles are distributed into the center of the cyclone where the gas is also injected in such a way to create a strong swirl responsible for both the heat exchange and the solid-gas particles separation. After that, the solid particles are deposited in the recovery tank below while the gas flows out from the upper part of the cyclone.

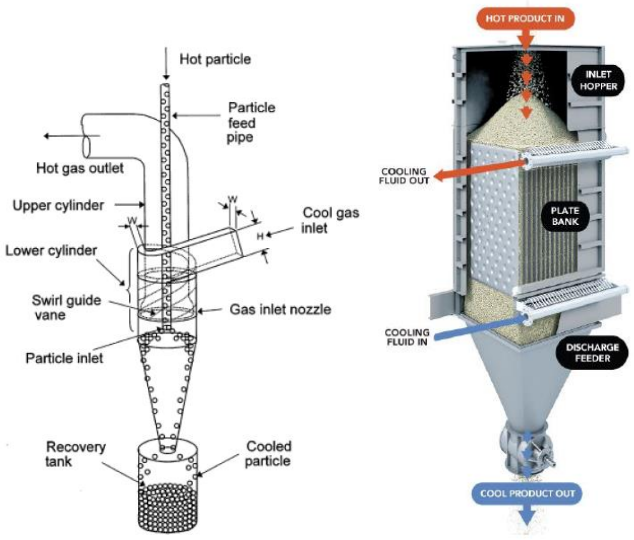

Figure 8. Direct-contact and indirect-contact cyclone for gas-solid heat exchanger **(3) (4)**.

As regards the closed configuration, an advanced plate heat exchanger has been proposed for heating or cooling a solid stream through a fluid flow. The solid particles flow downwards by gravity and are inserted between the stainless steel plates inside which a fluid medium flows, thus the heat transfer occurs by conduction. In the CaL-CSP integration, a closed configuration heat exchanger is required to preheat the solid CaO particles entering the carbonator with a CO_2 exhaust flow since a possible contact would partially initiate the carbonation reaction (5). A scheme of the structure and the inlet and outlet streams of the direct and indirect configurations is shown in Fig. 9.

Finally, a proposed technical solution for heat exchange between solids consists in connecting two gas-solid heat exchangers in parallel so that the fluid medium transfers the heat from the hot solid to the cold one passing from one exchanger to the other (4). Among heat transfer media, liquid metals can be used in the solid-solid configuration as they guarantee operation at high temperatures (5).

2.4 Solid conveying

A fundamental role in the CaL process is played by solid particles carrier through which the correct operations of the reactors are guaranteed by an adequate transport of solid reactants and products. In general, the transport mechanisms are based on pneumatic or mechanical conveying or by gravity depending on the size and temperature of the solid particles, on the required transport speed and finally on the available space (3) (4).

Being a mature and reliable technology, pneumatic conveying results the most suitable option for SOCRATCES project. The technique of pneumatic conveying consist in transporting the solid powders through a gas flow, promoted by fans, blowers or compressors that regulate the velocity and pressure of the gas entering the reactors or the gas-solid separators (4). The pneumatic conveying features, functional to the SOCRATCES project, are the rapid transport of powder and granular particles with a diameter up to about 50 mm, the improvement of the gas-solid heat exchange in the preheating phase, the flexibility in transport orientation, e.g. vertical, horizontal, etc., and the adaptability to both open and closed configurations (3). Two pneumatic conveying models has been considered: the dilute phase conveying and the dense phase conveying (3). In the first model, the solid powders are suspended inside a gaseous flow which transports them inside the pipeline of the conveying system. In order to ensure the particles suspension of most materials, the minimum gas velocity must be between

13-15 m/s, with a consequent high energy consumption of the device. The second models differs from the previous one because the solid particles are no longer suspended due to the low gas velocity. In fact, solid powders in the form of plugs are transported by a gas that pass through the spaces between the pelletized material (3). Given the low gas velocity, the energy consumption of dense phase conveying is clearly lower than the dilute phase one. On the other hand, the most significant disadvantages are represented by the limited number of materials used in the dense phase model and by the necessity to pressurize the gas in order to avoid pressure drop between solid and gaseous flows (3).

In the end, dense phase pneumatic conveying has been proposed for SOCRATCES project. The particle size of the Ca-based materials remains below 50mm, typical of cohesive powders. However, the fluidization of ultrafine powders is a critical aspect of pneumatic conveying, whose mobility is hindered by the tendency of the powders to create matter aggregates (3). In addition to the use of silica additives, several solutions are under investigation to reduce powders cohesion, including the sonoprocessing technique. An intense acoustic field is applied to the fluidizing flow to overcome the adhesion forces of the cohesive aggregates and, at the same time, the superposition of sound waves generates a greater gas fluctuation fostering fluid recirculation (3).

2.5 Gas Turbine

The technologies used for gas expansion and compression are well known, fully developed and reliable. In the CaL-CSP integration plant they are used for the treatment of CO_2 at high pressure and temperature. Thermal cycles should be kept as simple as possible avoiding reheating or intercooling stages despite the opportunity to improve the overall thermal efficiency of the system.

In general, compact machines such as compressors, combustors and turbines for process fluids are used in power cycles, resulting in economic savings and improved performance.

Chapter III

Power Cycle Models for CaL-CSP Integration

In this section, an overview of the several layouts of the CaL-CSP plant investigated so far is proposed in order to analyse the performance of the coupled thermochemical energy storage system with a power cycle. Then, the optimal configuration suggested by recent study will be presented by focusing on the plant layout and on the mass and energy flows involved in the CaL process.

2.1 Power Cycle Integration models

Considering the main Calcium Looping features as energy storage system, several CaL-CSP integration alternatives for power production have been proposed in recent studies. The purpose of this section is to explore the different CaL-CSP plant configurations focusing on the power cycle integration model in the carbonator zone. As mentioned before, the CaL process provides high temperature thermal energy that must be converted into electricity by means of a proper thermodynamic cycle. Based on whether the power cycle integration is open or close, two different process-integration approaches are defined: the direct and the indirect configurations.

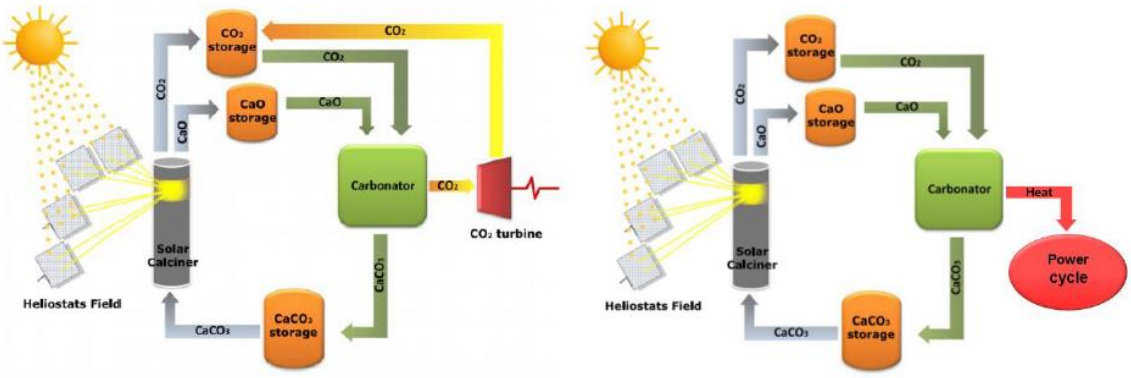

Figure 9. Diagram of power cycle integrations in the CaL-CSP plant (direct and indirect) **(9)**.

2.1.1. *Direct integration*

The main feature of the direct configuration is that the working fluid of the power cycle coincides with the CO_2 involved in the carbonation reaction, so inevitably the power cycle is directly connected to the carbonator zone. Through a multi-stage expansion, the pressure and temperature of the CO_2 are increased with respect to its storage conditions. Moreover, before entering the carbonator, both CO_2 and CaO are preheated by the reaction products exiting the chemical reactor. In order to guarantee a more efficient thermal control of the carbonator, the amount of CO_2 introduced in the carbonation environment is higher than that required to sustain the exothermic reaction. The excess of CO_2 leaving the carbonator is sent to the gas turbine for electricity production and then recalculated in the closed cycle. The following figure shows a simplified scheme of the direct close-cycle configuration for CaL-CSP integration.

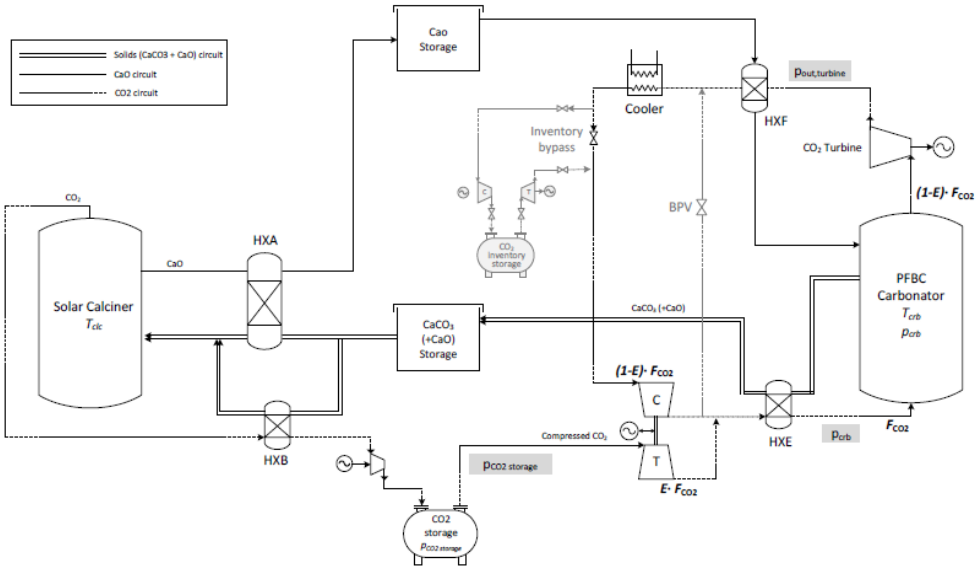

Figure 10. CO_2 closed configuration for direct integration in the CaL-CSP plant **(3)**.

An alternative configuration to the closed CO_2 cycle for direct integration was proposed in previous work, that is the air/CO_2 open cycle (3) (4). Differently from the CO_2 closed cycle configuration, the thermal energy released by the exothermic carbonation reaction is transferred to an air stream used as a working fluid in an open Joule-Brayton cycle (7). In fact, a mixture of air and CO_2 in stoichiometric quantity is introduce in the carbonation reactor so that the CO_2 reacts completely with the CaO, which after being extracted from storage condition at 1 bar and 20°C and is preheated (9) . As a consequence, the reaction products leaving the carbonator are $CaCO_3$ and pure air at

high temperature. The hot air stream is initially sent to a gas turbine to produce useful power, performing an open Joule-Brayton cycle (3). The temperature at which the exhaust air leaves the expansion turbine is such as to allow heat recovery through a heat exchangers network: the thermal energy released by air is used to pre-heat the solid reactant entering the carbonator. After the heat exchange, the air stream can be released into the external environment (3) (7). However, the equilibrium conditions of the carbonation reaction constitute a substantial constraint to the feasibility of air/CO_2 open cycle. According to previous studies, the main issue is related to the inevitable presence of CO_2 among the products of the carbonation reaction due to the thermodynamic conditions of the reactor. The CO_2 concentration among the gaseous products exiting the carbonator depends on the amount of CO_2 present into the carbonation environment. In fact, the carbonation reaction is interrupted when the CO_2 partial pressure in the carbonator is reduced to the equilibrium partial pressure imposed by the reactor temperature, causing the presence of non-reacted CO_2 in the carbonator (7). In order to minimize the CO_2 concentration in the exhaust gas, the carbonator should work at very high temperature and pressure conditions that are extremely difficult to sustain from a technological point of view. For this reason, the air/CO_2 Brayton cycle is no longer considered a valid option for power cycle integration, since the configuration efficiency is strongly limited by the low operating pressures achievable (3). For completeness, the layout of CaL-CSP plant with the process-integration based on the air/CO_2 open cycle is shown in the Fig.11.

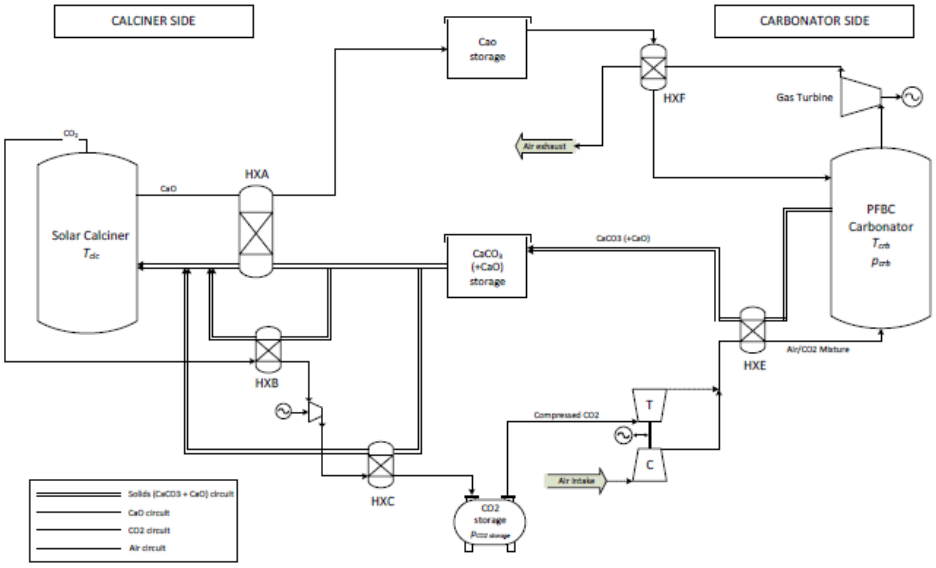

Figure 11. Direct integration configuration based on an air/CO_2 open Brayton cycle for CaL-CSP plant **(3)**.

2.1.2. *Indirect Integration*

The indirect integration model is based on the physical separation between the power cycle and the carbonator system, which are therefore connected through a heat transfer fluid. The thermal energy is extracted from the carbonator, recovered by means of a heat exchanger and then released to the power cycle. The indirect integration has numerous advantages, including the adaptability to supercritical CO_2 cycles as the technological solutions adopted allow to operate in a wider range of temperatures and pressures compared to the direct configuration (3). In addition, different thermodynamic cycles and working fluids can be used for power production depending on the amount and temperature of thermal power available. As already mentioned, the working fluid of the SOCRATCES power cycle consists exclusively of CO_2, so a higher quantity than the stoichiometric one is introduced in order to ensure that a non-reacted portion of CO_2 flows out of the carbonator. In Fig.12 is shown the layout of the indirect cycle configuration.

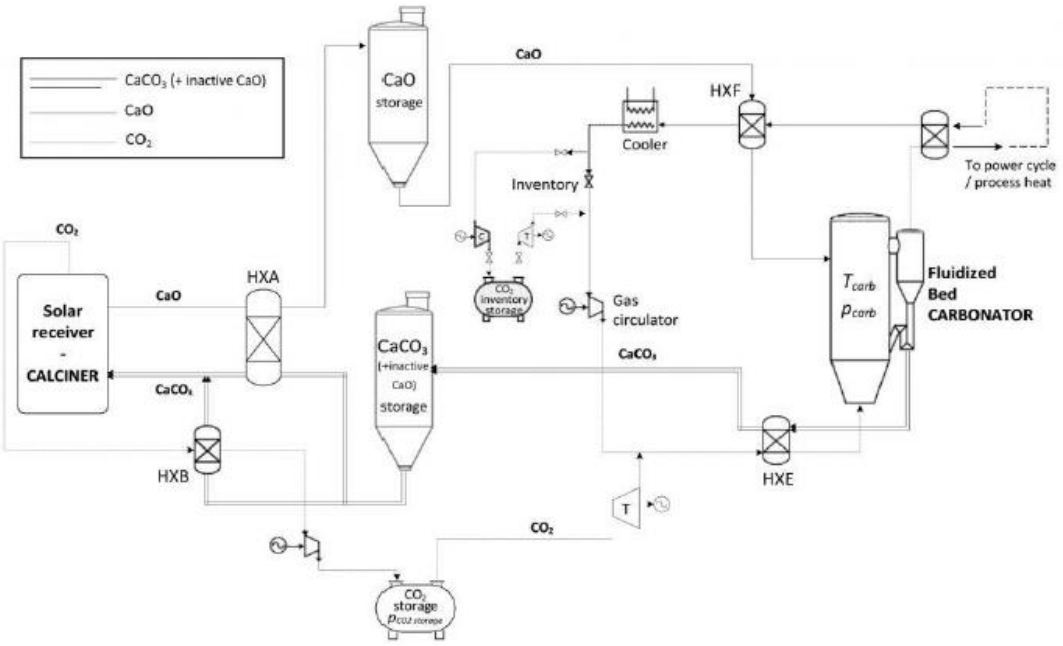

Figure 12. Closed CO_2 cycle for indirect integration of the CaL-CSP plant **(4)**.

In general, the CO_2 closed cycle both for direct and indirect configuration requires a more complex plant design that concerns the heat exchanger network and the power cycle equipment. A closed-loop cycle requires the addition of specific components, such as storage system, compressor and expander in order to guarantee the process fluid recirculation. As shown in Fig.12, the indirect configuration layout presents an inventory storage system that regulates the circulating mass flow of CO_2 based on the

loads variation during the plant operation (3) (4). In order to ensure the proper operation of the CO_2 storage system, a compressor and a turbine are required to change the pressure of the circulating gas flow in closed loop cycle based on the value of the storage pressure, that is approximately 75 bar at 20°C (3). Although the control systems determine a reduction in the overall plant efficiency, the closed cycle configuration represents the most suitable solution for the integration of the power cycle since the carbonator pressure can reach high values such as to determine high carbonation temperature and consequently greater efficiency (3).

As seen in the layouts proposed for the power cycle integration, the plant configuration includes not only the carbonator side but also the calciner one, which on the contrary remains unchanged for both direct and indirect integration. The reason why the calciner section shows the same configuration for each power cycles approach is found in the physical and operational separation of the two parts of the plant by means of the storage vessels placed between them. In fact, the charging and discharging phases of the CaL storage system take place respectively in the calciner, in which solar energy is supplied, and then in the carbonator, where thermal energy is produced and transformed into electricity (3).

2.2 Mass balances

The main features of the CaL-CSP integration model in terms of mass and energy balances for the different components are outlined in order to provide a more efficient plant configuration (7). As already mentioned, the operational separation of the plant between the calciner and carbonator side thanks to the storage systems installation necessarily determines different mass and energy flows involved in the two parts of the plant. The diagram of the mass flows involved in the CaL process is shown in Fig.13. The recirculating solid stream leaving the carbonator $F_{R,carb}$, formed by the carbonation product $CaCO_3$ and the CaO unreacted fraction is delivered to the calciner, where the $CaCO_3$ solid particles complete the decomposition process (7). The calcination reaction of a mole of $CaCO_3$ gives rise to a mole of CO_2 and a mole of regenerated CaO, which in turn constitutes the solid stream exiting the calciner together with unreacted CaO. The solid and gaseous output streams of the calciner are sent to the carbonator where a part of CaO reacts with CO_2 to produce solid $CaCO_3$ while the remaining unreacted part leaves the carbonator among the solid products, and so the loop is completed. Finally,

the stream indicated in the scheme with F_{heat} consists of a CO_2 flow used as heat transfer fluid for the thermal energy produced during the carbonation reaction in order to perform a power cycle closed integration (7).

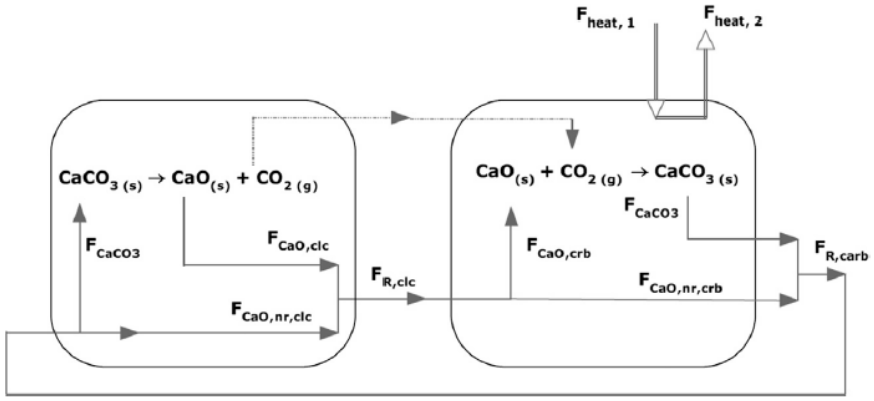

Figure 13. Mass-balance scheme for CaL process **(7)**.

Once the mass flows circulating in the two regions of the plant have been identified, an assessment of streams availability in a specific time period is required in particular for the storage systems sizing. The solar calciner operations are strictly connected to the solar energy supply, daytime period and clear sky conditions, while the carbonator must provide thermal power continuously. Therefore, the storage systems must be sized in order to enable the carbonator/turbine group to operate for a baseline period of 24 hours, adapting to the load variations based on the energy demand (3) (7). Considering an average period of 24 hours, the $CaCO_3$ amount required to support the stationary plant operations can be found by solving the following mass balance equation (7):

$$\int_{24h} F_{CaCO3,clc}(t)dt = \int_{24h} F_{CaCO3,crb}(t)dt$$

where $F_{CaCO3,clc}$ and $F_{CaCO3,crb}$ are the amount of the $CaCO_3$ respectively decomposed in the solar calciner and produced by the carbonation reaction for power generation that must be equal in the reference period. The molar flow rates are considered constant and equal to the integral average value over the daytime period thus determining an average plant performance. The average daytime period h_{sun} corresponds to the hours during which the solar energy collected by the CSP application is supplied to the calciner in order to drive the endothermic calcination reaction (3). As a consequence, the mass-balance equation can be reduce to the following expression:

$$\overline{F_{CaCO3,clc}} \cdot h_{sun} = \overline{F_{CaCO3,crb}} \cdot 24$$

so that the ratio between the average molar flow rates circulating in the calciner side and the carbonator side depends only on the operating time of the two reactors. Assuming a daily solar availability of 8 hours (h_{sun}), the average ratio between the molar flow rates over a 24-hour period is equal to 3, which means that the flow rate circulating in the calciner is three times greater than that circulating in the carbonator (3). As previously mentioned, the aim of the presented mass-balance model is to determine the storage vessels size for the materials involved in the CaL process. In fact, an effective plant performance control strategy requires a more complex mass balance model based essentially on the load curve and weather conditions.

2.3 Energy balances

The CaL process clearly involves energy flows both in calciner and carbonator side, which can be analyzed using an energy balance model. In general, the energy balance equation for an open system during steady-state operation, valid in this case for a chemical reactor, can be expressed as:

$$\sum_i F_{i,out} h_{i,out} - \sum_i F_{i,in} h_{i,in} = \Phi - \dot{W}$$

where Φ and $\dot{W}$ are the thermal and the mechanical powers of the system exchanged with the external environment while F_i and h_i are respectively the molar flow rate and the molar enthalpy of the inlet and outlet streams (3) (7). Since the CaL process is based on chemical reactions, it is necessary to define thermo-chemical parameters, such as the reaction rate ξ and the stoichiometric coefficient ν_i of the compound, in order to evaluate the variation of the components amount during the reaction phases according to the following equation: $F_{i,out} - F_{i,in} = \xi \nu_i$ (3). Moreover, the reaction enthalpy variation at the reaction temperature can be define as $\Delta H_R(T_{react}) = \sum_i \nu_i h_i$ (3). Considering the chemical reaction parameters, the energy balance equation can be written as follows:

$$\xi \Delta H_R(T_{react}) + \sum_i F_{i,in}(h_{i,react} - h_{i,in}) = \Phi - \dot{W}$$

while the first contribution represents the reaction heat associated with the energy change in the control volume, the second the heat necessary to bring the reactants into the reactor conditions (3). The energy balance equation obtained is applied to both reactors which theoretically operate in isothermal conditions. The energy balance model implemented for the calciner side allows to evaluate the amount of $CaCO_3$ that must be

introduced into the reactor so that the absorbed energy is exploited not only to perform the reaction, but also to preheat the solid inlet stream up to the calcination temperature (3). However, the absorbed solar energy is supplied to the calciner net of non-negligible energy losses due to convection, radiation, absorption and reflection. The incoming and outgoing energy flows for the calciner are shown in the Fig. 14.

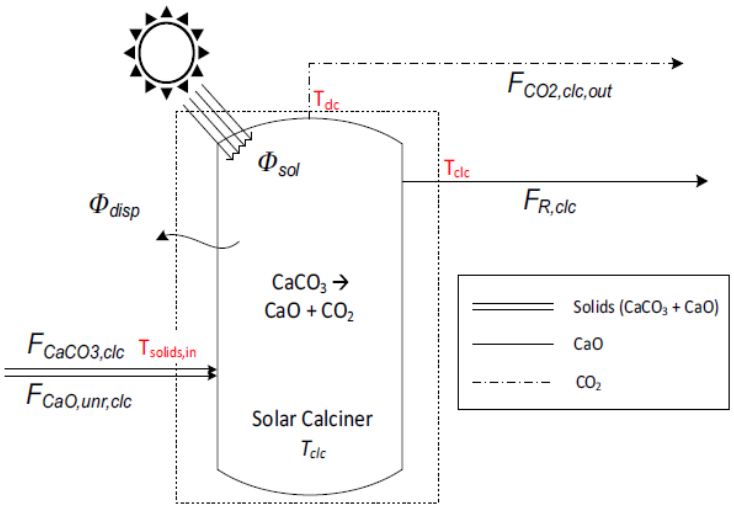

Figure 14. Energy balances for the calciner side **(3)**.

On the other side, the carbonator energy balance model is used to determine the amount of CO_2 required both to make the reaction take place and to remove heat from the reactor considering though the energy dispersed by the walls and used to preheat the reactants. The energy flows for the carbonator are shown in the Fig. 15.

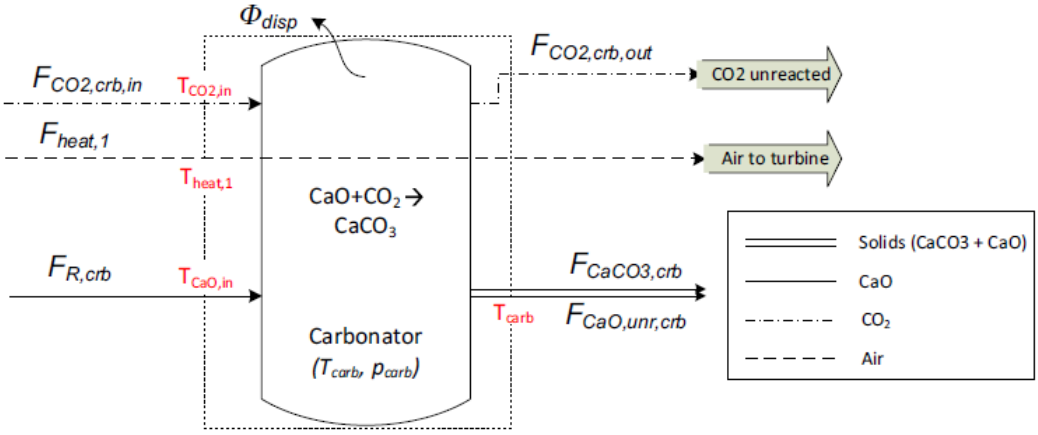

Figure 15. Energy balances for the carbonator side **(3)**.

Chapter IV

Methodology: Application of Pinch Analysis for CaL-CSP plant

In general, the industrial processes require energy for heating and cooling simultaneously which can be provided by creating a heat exchangers network that uses process flows. Therefore, the hot fluids cool down releasing heat which in turn is transferred to the cold fluids which instead heat up (10). The methodology used to design the heat exchanger network is the pinch-analysis which creates a plant configuration capable of minimizing energy consumption from external resources by exploiting those internal to the system (7). Based on the minimum temperature approach between hot and cold streams, the ΔT_{min} of the heat exchangers must be chosen in such a way as not to result in too high heat exchange surfaces. In general, depending on the production process, a different reference value can be identified: for chemical processes ΔT_{min} is equal to 20°C (10). The data assumed for the Pinch-Analysis concerning the value of operating parameters, such as the carbonation temperature and pressure, the CaO reactivity X and the outlet pressure of the CO_2 turbine (7) are taken from the Alovisio et al. 2015 (3) and discussed below.

The first step of pinch-analysis consists in the identification and characterization of the process streams, as regards the temperature at which they are available, the temperature at which they must be brought and their mass flow rate.

Once the optimal values of the parameters listed above have been identified, the overall plant efficiency can be further improved by means of a thermal optimization based on a heat recovery system.

Starting from the calciner side, the inlet and outlet streams involved in the process are:

- The $CaCO_3$ solid stream which leaves the storage system at ambient temperature conditions and must be heated before entering the calciner

- The CaO stream and the CO_2 stream which constitute the calcination products at high temperature exiting the system which instead must be cooled down to ambient temperature before being stored.

On the other hand, the carbonator side system is characterized by:

- The CaO and the CO_2 inlet streams coming from their respective storage vessels
- The $CaCO_3$ outlet stream as carbonation process product together with the excess CO_2 stream.

An essential parameter to perform the pinch analysis is the product between the mass flow rate and the specific heat of the stream $Gc_p\left[\frac{kW}{k}\right]$, which provides indication on the stream thermal capacity and on the energy amount that is able to transfer in the unit of time. Although some process fluids vary in a wide temperature range, in the pinch-analysis the Gc_p product is considered constant since the specific heat is averaged between the extreme temperatures assumed by the stream (3). As mentioned before, the mass flow rate of each stream is calculated by applying the equations of the mass and energy balances, taking into account its dependence on time and on the solid reactivity *X*, which determines the amount of unreacted CaO in the CaL process (3). In the Alovisio et al. 2015 (3) study the mass flow rates of each stream were assessed for different values of solid reactivity *X*. For the purpose of this analysis, it is sufficient to consider the CaO conversion equal to *X*=0.2 since high plant efficiency of the CaL process are already achieved (7). In fact, the Fig. 16 shows how the efficiency of the system in the different configurations analyzed in Alovisio et al. 2015 (3) as a function of the CaO solid reactivity does not undergo evident variations for values between X = 0.2 and X = 0.5.

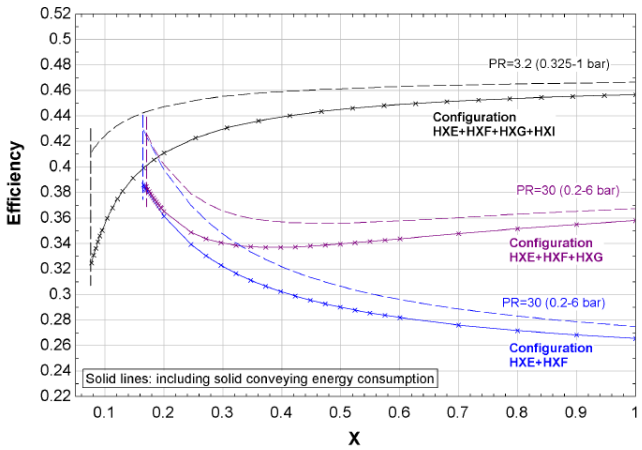

Figure 16. The efficiency curves for the three different configurations simulated in the Alovisio work with respect to the CaO solid reactivity **(3)**.

Once the mass flow rates of the carbonator system streams have been determined, the mass flow rate of the streams participating in the calcination reaction is calculated by means of the mass balance equation, taking into account the operating hours of both the solar calciner and the carbonator systems. As shown in the direct configuration scheme of the CaL-CSP system in Fig. 17, the process streams are available for a different time duration depending on the system to which they belong.

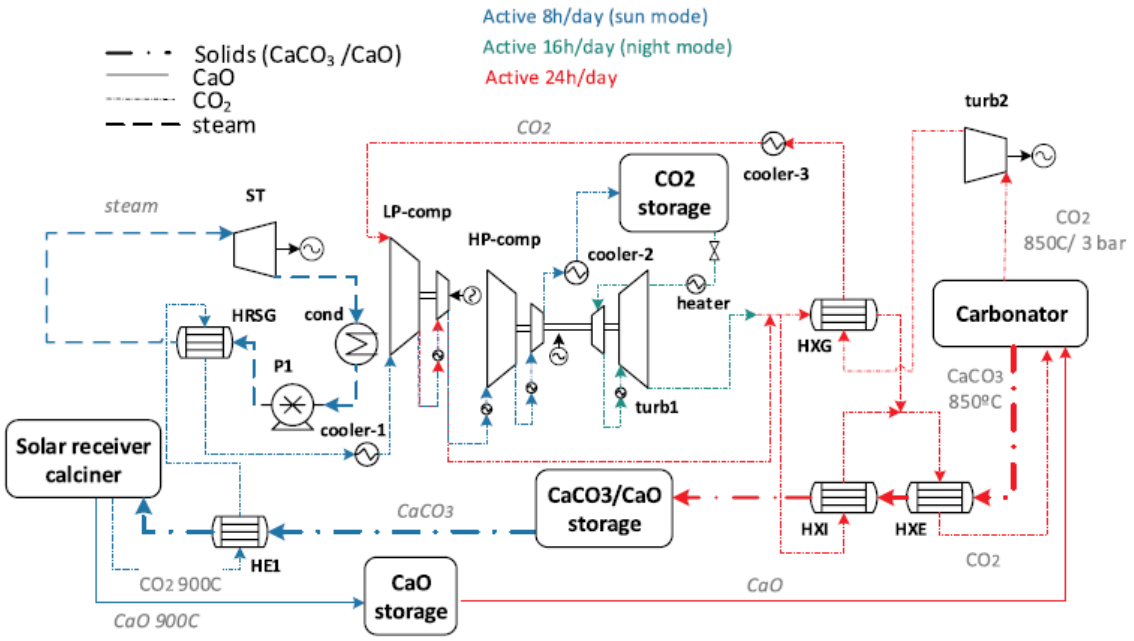

Figure 17. CaL-CSP system in direct configuration with the process streams available in different times according to the duration of the charging and discharging phase of the energy storage **(5)**.

The data used in this discussion are extracted from the simulations performed by the Alovisio et al. 2015 (3). Assuming that the solar radiation is available for 8 hours a day (h_{sun}), the mass flow rates of the solar calciner must be calculated in such a way that the charging process is able to sustain the discharge process continuously for 24 hours by means of the equations derived from the mass balance model:

$$\overline{F_{CaCO3,clc}} = 3 \cdot \overline{F_{CaCO3,crb}}$$

$$\overline{F_{CaO,clc}} = 3 \cdot \overline{F_{CaO,crb}}$$

while the CO_2 mass flow rate is calculated as the difference between the inlet $CaCO_3$ mass flow rate and the outlet CaO one from the solar calciner:

$$\overline{F_{CO2,sens,clc}} = \overline{F_{CaCO3,clc}} - \overline{F_{CaO,clc}}$$

The results obtained through the mass balance calculations are reported in the Table 2.

Carbonator side		Calciner side	
Streams	$\dot{m}$ $[kg/s]$	**Streams**	$\dot{m}$ $[kg/s]$
$CaCO_3$	88,5	**$CaCO_3$**	265,5
CaO	76,5	**CaO**	229,5
$CO_{2,out\ turbine}$	73,8	**$CO_{2,sensible}$**	36,0
$CO_{2,out\ compressor}$	85,8	**$CO_{2,compressor}$**	36,0

Table 2. Mass flow rates of both the carbonator and the calciner side considering the different duration of the charging and discharging phase in the CaL process.

In order to perform the pinch-analysis, the temperature range of each process flow must be defined, in particular the temperature at which it is made available and the one that must reach. Thus, the process streams will be divided between hot fluids from which it is possible to extract thermal power and cold fluids to which heat is supplied. In this way, the network of heat exchangers is able to minimize the energy requirements from external resources, thus exploiting the internal ones. Starting from the data found in Alovisio et al. 2015 (3), the CaL process streams in the closed CO_2 cycle for direct integration require some considerations from the thermal point of view. In the calciner side the temperature target required are:

- the inlet stream composed by the $CaCO_3$ and the unreacted portion of CaO ambient condition T_{amb} must be heated up to the calcination temperature T_{clc}
- the CaO stream leaves the solar calciner at T_{clc} and must be brought to ambient conditions T_{amb} in order to be stored
- the CO_2 sensible stream must be cooled possibly down to ambient temperature T_{amb}, since it must be subsequently compressed to reach the storage pressure
- the CO_2 compressed stream become a hot flow available at the compression outlet temperature $T_{comp,out}$ for heat exchange and as well as the CO_2 sensible stream must be brought to ambient temperature.

On the other side, the target temperature of the carbonator inlet and outlet streams has been assessed considering:

- the cold CaO stream, entering the carbonator, must be heated up to the temperature as close as possible to the carbonator temperature T_{carb},
- the cold inlet CO_2 stream, as well as the CaO stream, should possibly reach the carbonation temperature
- the hot $CaCO_3$ solid stream, leaving the carbonator at T_{carb}, must be cooled down to the ambient temperature T_{amb}

- the hot CO_2 flow leaving the carbonator is first sent to a gas turbine and then made available for heat exchange at the outlet temperature $T_{turb,out}$ of the turbine and must be brought back to ambient conditions T_{amb}.

The fixed parameter conditions for a closed CO_2 power cycle in case of direct configuration have been evaluated on the basis of previous considerations regarding the operating conditions of the CaL plant. The calcination temperature T_{clc} is set equal to 900°C, the carbonator temperature T_{carb} at 875°C, the ambient temperature is equal to 20°C. The outlet compression temperature $T_{turb,out}$ in the calciner side calculated through a simulated analysis is equal to 474°C. The results are summarized in the Table 3. and Table 4. respectively for the calciner and the carbonator side.

Calciner Streams		***Type***	$\boldsymbol{Gc_p\left[\frac{kW}{k}\right]}$	$\boldsymbol{T_{in}[°C]}$	$\boldsymbol{T_{out}[°C]}$
1	CaO	Hot	219,15	900	20
2	Solids ($CaCO_3$+CaO)	Cold	271,35	20	900
3	CO_2 sensible	Hot	42,32	900	20
4	CO_2 compressed	Hot	39,21	474	20

Table 3. Stream identification for the calciner side **(3)**.

Carbonator Streams		***Type***	$\boldsymbol{Gc_p\left[\frac{kW}{k}\right]}$	$\boldsymbol{T_{in}[°C]}$	$\boldsymbol{T_{out}[°C]}$
5	CO_2 out, turbine	Hot	75,3	426	20
6	CO_2 out, compressor	Cold	94,65	20	875
7	CaO	Cold	65,92	20	875
8	Solids ($CaCO_3$+CaO)	Hot	87,35	875	20

Table 4. Stream identification for the carbonator system **(3)**.

Before designing the network of heat exchangers, the maximum and minimum thermal energy requirements must be calculated in order to evaluate both the amount of energy required by the system and the energy saved through heat recovery (10). The maximum energy requirements can be evaluated by adding separately the thermal powers of the hot and cold streams. On the other hand, the minimum energy requirements can be assess though a graphical method in which the Composite Curves of thermal power of cold and hot streams are constructed separately as a function of the temperature. In general, heat recovery can only occur if the curve corresponding to hot fluids is greater

than that of cold fluids. Then, the cold composite curve is moved horizontally to reach the minimum approach temperature between two points of the hot and cold curves with the same abscissa. In the Fig. 18 and Fig. 19 are reported the composite curves for both calciner and carbonator system.

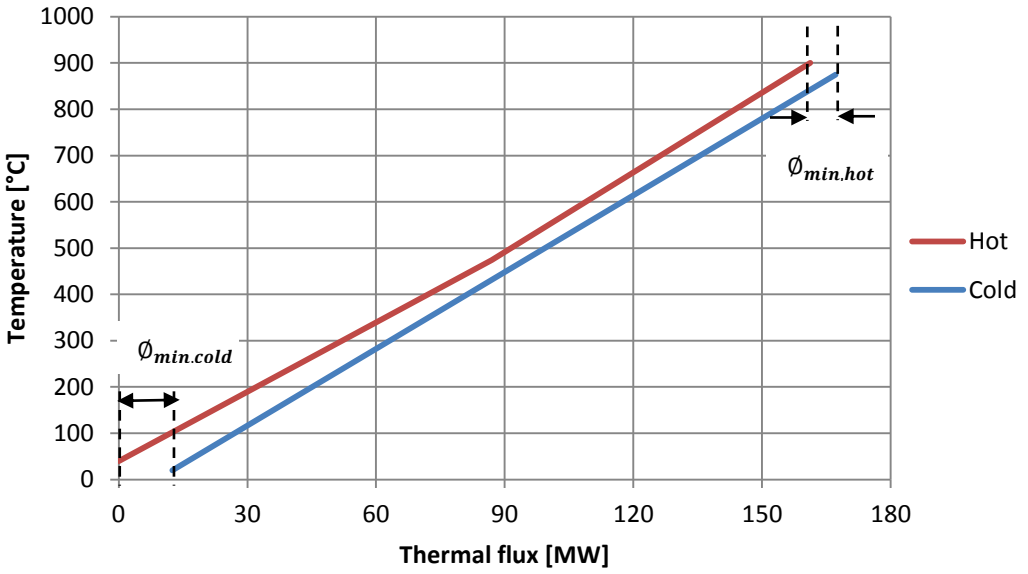

Figure 18. Composite curve for calciner side streams obtained from the pinch-analysis both for hot streams and cold streams when the CaO conversion is X=0.20.

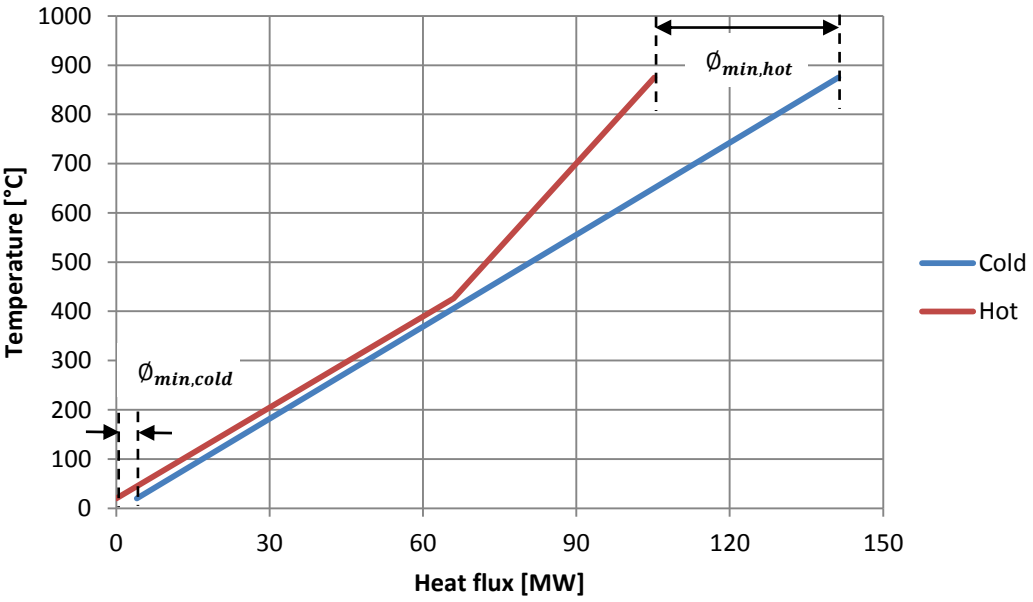

Figure 19. Composite curve for carbonator system streams derived from the pinch-analysis both for hot and cold streams when the CaO conversion is X=0.20.

As shown in the Fig. 18, the calciner side has a lower minimum heat and cooling requirements compared to the carbonator side. The cold composite curve coincides with the thermal power that can be extracted from the only cold fluid in the calciner, i.e. the

$CaCO_3$ solid stream, while the hot composite curve consists of the three hot fluids involved. On the contrary, as shown in the Fig.19, additional external heat is needed to heat up the cold streams in the carbonator side, since the reactants have to reach the carbonation temperature. Moreover, the cooling requirements are smaller than the heating ones.

The minimum requirements for heating and cooling can be also calculated by means of the analytical method for the pinch-analysis through which the temperature of the pinching point is easily found, i.e. the temperature in which the minimum temperature between the hot and cold composite curves occurs. As mentioned before, the minimum temperature approach ΔT_{min} for the pinch-analysis is set at 20°C.

The analytical method first step is the determination of the shifted temperatures for both hot and cold streams extreme temperatures as follows:

$$\left(T_{shifted}\right)_{hot} = T - \frac{\Delta T_{min}}{2}$$

$$\left(T_{shifted}\right)_{cold} = T + \frac{\Delta T_{min}}{2}$$

The shifted temperatures thus obtained are ordered in decreasing order. Then, for each temperature range the available net heat flows are calculated by adding the heat capacity of the hot streams and subtracting the heat capacity of the cold streams and finally multiplying the Gc_p thus obtained by the difference between the shifted temperatures of the considered interval. After that, the net thermal flux of each interval is added to the sum of the previous intervals in order to obtain the Infeasible Heat Cascade showing in which interval heat surplus or deficit occur. The minimum value of thermal flux obtained in the Infeasible Heat Cascade is then insert in the first temperature interval of the next Heat Cascade thanks to which the minimum requirement of heating and cooling are determined. The first term of the Heat Cascade represents the minimum heating requirement, while the last one refers to the minimum cooling requirement. Furthermore, the interval in which the Heat Cascade is zero corresponds to the pinch-point, i.e. where the temperature between hot and cold fluids is minimal (10).

In the following table are summarized the maximum and minimum requirements for heating and cooling in the CaL-CSP integration process assessed with the pinch-analysis through the analytical method.

Energy Requirements	*Maximum Heating [MW]*	*Maximum Cooling [MW]*
Calciner	238,79	247,89
Carbonator	137,29	105,26

Table 5. Maximum energy requirements for calciner and carbonator systems.

Energy Requirements	*Minimum Cooling [MW]*	*Minimum Heating [MW]*
Calciner	18,74	9,64
Carbonator	4,06	36,09

Table 6. Minimum energy requirements for calciner and carbonator systems.

After assessing the conditions of the pinch-point, the optimal configuration of the heat exchanger network can be determined in such a way as to make the portion of the plant above the pinch-point energetically independent from that below, avoiding the heat exchange between the two parts.

In order to trace the network that allows to minimize external energy requirements taking into account the previous consideration, it is necessary to follow some practical rules:

- Above the pinch-point, the number of cold streams must be greater or equal to the number of hot streams as well as the product Gc_p

$$N_{cold\ stream} \geq N_{hot\ stream}$$

$$Gc_{cold} \geq Gc_{hot}$$

- Below the pinch-point, the number of hot streams must be greater or equal to the number of cold streams as well as the product Gc_p

$$N_{hot\ stream} \geq N_{cold\ stream}$$

$$Gc_{hot} \geq Gc_{cold}$$

In general, it is possible to increase the number of hot or cold streams in order to respect the constraints just reported above, by spitting the streams and the respective products Gc_p both for the part of the plant above and below the pinch-point.

- Each heat exchanger must respect the minimum approach temperature between the inlet and outlet temperatures of the thermal component, therefore the inlet and outlet temperatures of the hot stream must be greater than at least ΔT_{min} compared to those of the cold one, having considered countercurrent operation for the heat exchanger.

Furthermore, the construction of the network of heat exchangers requires the determination of the thermal power available for each temperatures interval of the entire process by simultaneously considering hot and cold fluids for each of them. Contrary to what is represented in the Composite Curves, an unique Grand Composite Curve is obtained through which the minimum heating and cooling requirements and the pinch-point temperature of the system considered are reported. The temperature at which the thermal flux is null corresponds to the pinch-point one.

3.1 Pinch-analysis for Calciner side

Based on the previous consideration, a network of heat exchangers for both calciner and carbonator side is proposed in which hot and cold streams are coupled according to the presented practical norms.

The Grand Composite Curve for the calcination system is reported in the Fig. 20. The resulting pinch-point temperature for the hot streams is equal to 474°C while for the cold streams is 454°C.

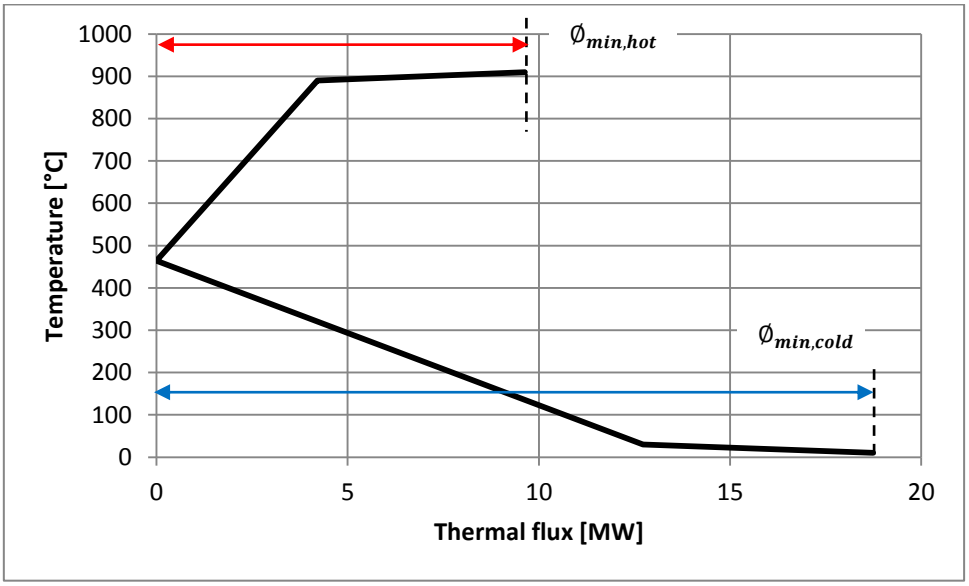

Figure 20. Grand Composite Curve for calciner side derived from the pinch-analysis.

The resulting heat exchangers network for the calciner side can be represented as follows, considering the data reported in the Table. 3:

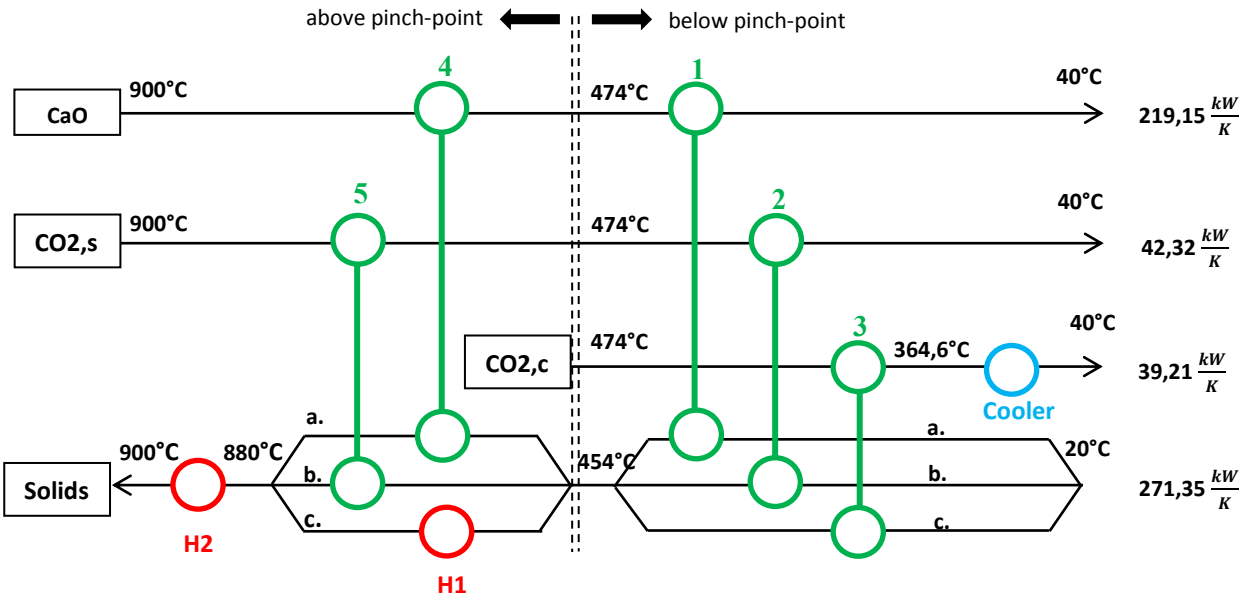

Configuration – Calciner side

As shown in the configuration of the heat exchangers, in the part of the system below the pinch-point the only cold stream ($CaCO_3$+CO_2 solid stream) is splitted into three different flows with lower thermal capacity Gc_p so that they can be coupled with three hot streams available. In the same way, in the part of the plant above the pinch-point the cold fluid was divided again into three flows to be coupled with the two hot fluids and finally heat the remaining part of fluid through an external heater. The product Gc_p for the three splitted streams for the cold fluid are summarized in the table below.

Splitted streams	Gc_p*[kW/K]*
a.	219,15
b.	42,32
c.	9,88

Table 7. The splitted stream for the cold flow in the calciner side for the heat exchangers configuration following the pinch-analysis.

The heat exchanger thermal power can be calculated by means of the following expression, considering the thermal capacity and the temperature difference between the heat exchanger inlet and outlet so as to respect the constraint of the minimum temperature approach:

$$\emptyset_{HEX} = Gc_p \cdot (T_{out} - T_{in})$$

The thermal fluxes for each heat exchanger are summed up in the Table. 8, including the thermal fluxes exchanged with the external resources by means of cooler and heater.

HEX	*Gc_p[kW/K]*	*Tin [°C]*	*Tout [°C]*	*Thermal power [MW]*
1	219,15	474	40	**95,11**
2	42,32	474	40	**18,36**
3	39,21	474	40	**4,29**
4	219,15	900	474	**93,36**
5	42,32	900	474	**18,03**
Cooler	39,21	364,6	40	**12,73**
Heater 1	9,88	880	454	**4,21**
Heater 2	271,35	900	880	**5,43**

Table 8. Thermal powers of the heat exchanger for calciner side, considering also the external resources by means of the cooler and heater.

3.2 Pinch-analysis for Carbonator side

The same analysis is carried out for the carbonation system. The Grand Composite Curve is reported in the graph below (Fig. 21). The pinch-point temperature results 426°C for the hot streams, whereas equal to 406°C for the cold flows.

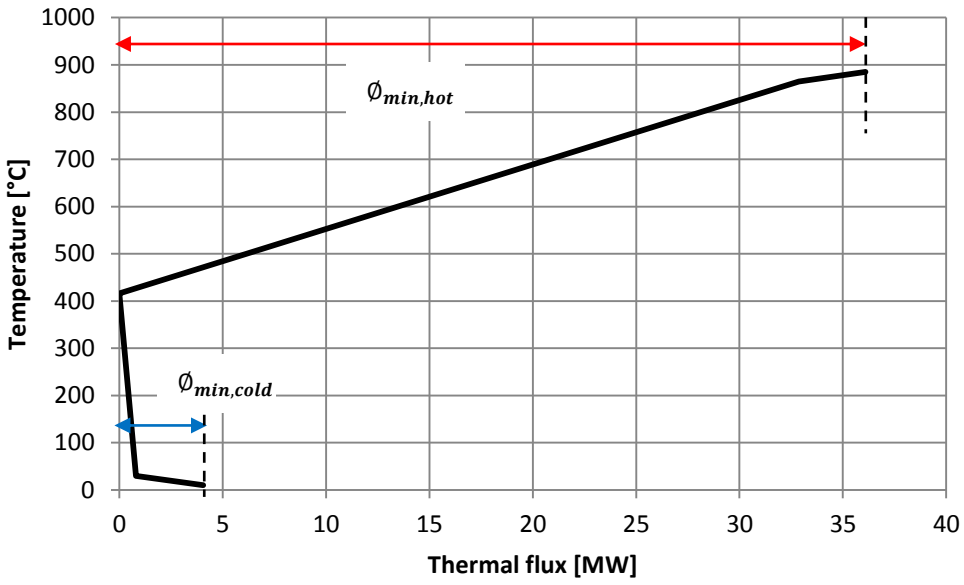

Figure 21. Grand Composite Curve for carbonator side derived from the pinch-analysis.

The resulting heat exchangers network for the carbonator side can be represented as follows, considering the data given in Table. 4:

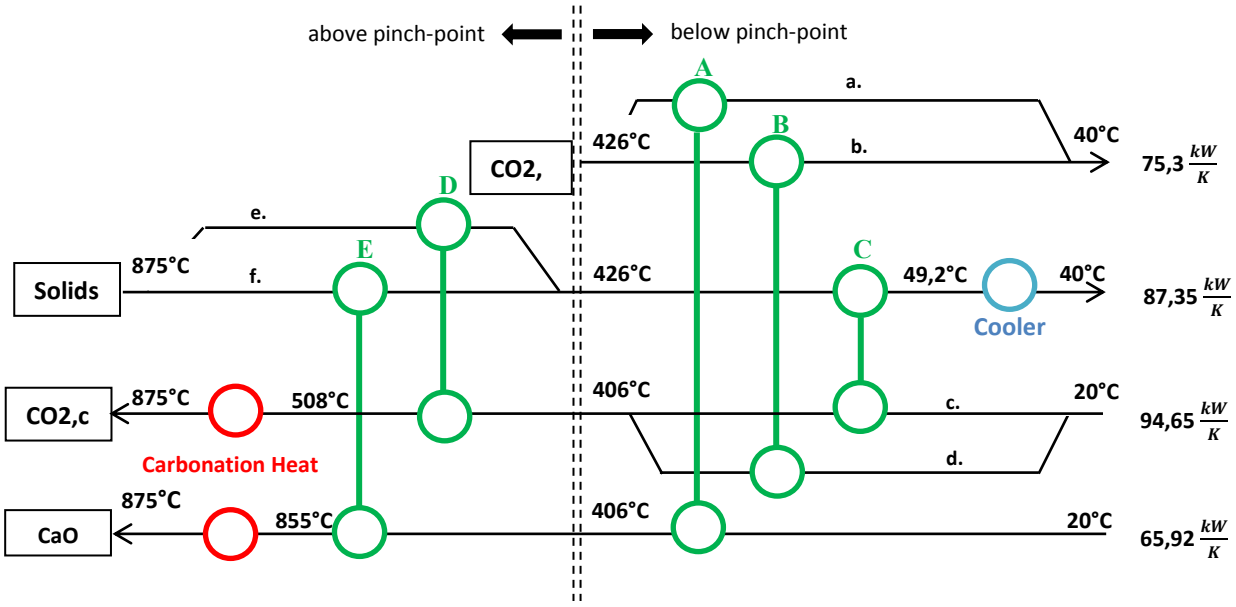

Configuration – Carbonator side

Below the pinch-point part of the plant, the number of hot flows involved in the process is equal to the number of cold ones. However, it is necessary to split both the cold and the hot CO_2 streams in order to respect the Gc_p product practical rule for pinch-analysis. On the other hand, in the part of the configuration above the pinch-point, the only hot stream is splitted in order to obtain the same number of cold and hot flows. The Gc_p product for each splitted stream has been calculated and reported in the Table. 9. Contrary to the configuration of the calciner side, the carbonator system is able to exploit the carbonation heat to meet the heating requirements without having to resort to additional heaters.

Above pinch-point		*Below pinch-point*	
Splitted streams	***Gc_p[kW/K]***	***Splitted streams***	***Gc_p[kW/K]***
e.	21,43	**a.**	65,92
f.	65,92	**b.**	9,38
		c.	85,27
		d.	9,38

Table 9. The splitted stream for the flows involved in the carbonator side following the pinch-analysis.

Once the Gc_p products have been assessed, the thermal power of each heat exchanger in the carbonation system can be calculated by applying the same equation used for the calcination system. The results are summarized in the table below.

HEX	Gc_p*[kW/K]*	*Tin [°C]*	*Tout [°C]*	*Thermal power [MW]*
A	65,92	426	40	**25,45**
B	9,38	426	40	**3,62**
C	87,35	426	49,2	**32,62**
D	21,43	875	426	**9,62**
E	65,92	875	426	**29,60**
Cooler	87,35	49.2	40	**0,80**
Heater 1	94,65	875	507,7	**34,76**
Heater 2	65,92	875	855	**1,32**

Table 10. Thermal powers of the heat exchangers for carbonator side, considering also the external resources by means of the cooler and heater.

The purpose of the pinch-analysis is to create a configuration of heat exchangers in such a way as to recover heat inside the system. Since the carbonator and calcination system are physically separated, the analyses were conducted in such a way as to keep the two parts independent of each other. In fact, the process streams of the calcination system carry out the heat exchange only between them, as well as for the carbonator system. Furthermore, the network of heat exchangers has been constructed in such a way as to foster the heat transfer between gas-solid or gas-gas wherever possible. However, it was necessary to insert solid-solid heat exchangers (7).

3.3 Pinch-analysis for batch-process

The pinch-analysis technique described so far deals with continuous processes in steady-state conditions. However, the pinch-analysis can also be applied to batch-processes considering the time-dependency of the system streams as explained in Kemp et al. 2006 (11). The advantages of batch-process analysis include both greater energy and cost saving opportunities and more efficient thermal recovery able to adapt to the different operating phases of the system. On the other hand, the analysis of discontinuous process presents numerous difficulties with respect to the continuous one due to the different availability in a given period of time and the variation in the thermal capacity of each stream. Despite the issues related to the methodology of the batch-process analysis, it allows to evaluate:

- the maximum heat exchange for each batch of the entire process
- the possibilities to introduce storage systems between batches
- the chance to reschedule the operational process to improve the heat exchange
- the design of heat exchanger network for these purpose.

The purpose of the following discussion is to describe the pinch-analysis methodology for batch-process in order to study the adaptability to the CaL-CSP integration. In general, continuous processes are characterized by the continuous presence of the process streams throughout the system's operating time. Each stream is therefore defined by several parameters that remain constant over the time period, such as the mass flow rate, the specific heat and finally both the supply and target temperatures.

On the contrary, the batch process is characterized by the presence of many process streams only in a certain time period. For this reason, one or more parameters that describe each process stream can no longer be considered constant. The used methodology identifies four basic types of streams:

- Type A streams are characterized by a fixed supply and target temperature, a fixed thermal load but a limited availability over a period of time. They are typically defined as flowing streams, in fact in the steady-state conditions correspond to the streams described in continuous processes
- Type B streams show a progressive variation of the thermal load despite the fact that both supply and target temperatures are fixed (e.g. the hot volatile product derived from batch reaction)
- Type C streams present a gradual change in temperature while the thermal load is kept constant (e.g. a liquid in a component heated by a constant thermal power)
- Type D streams are determined by changes in both temperatures and thermal loads over time and are typically the most common stream types for batch-process and the most complex to be treated (e.g. jacketed reactor heated by steam or cooled by water).

Once the types of flow that characterize the batch process have been identified, it is required to define the time intervals of the batch-process considering precisely the times in which the stream starts, ends or presents evident changes in the parameters already mentioned. The Time Interval-Method is easily applicable for Type A streams, but hardly adaptable to Type B, C and D streams due to thermal load and temperatures

changes in time. In fact, infinite time intervals would be necessary in order to consider these parameters constant. For this reason, practical approximations of the stream conditions should be introduced in such a way as to reduce all streams types to Type A. After separating the processing cycle into time intervals, each of them presents a different combination of streams in which conditions are assumed constant. Then by means of the Time Events Diagram it is possible to show which streams exist and in which time intervals. Therefore, for each identified time interval, a heat cascade calculation is performed to evaluate the hot and cold utility target in exactly same way for continuous processes. The hot and cold utility loads define the Maximum Heat Recovery for each time interval through direct heat exchange and whether they are plotted on a graph as a function of time, the Utility-Time Graph is obtained thanks to which it is possible to identify when the heat and cold utilities are required. Therefore this tool not only allows to evaluate the heat recovery in every time interval, but also offers the opportunity to perform a reprogramming of the batch process in order to limit the mismatch between the heat and cold requirements in the overall process cycle.

3.3.1 Batch-process analysis for heat exchanger network

Once the pinch-analysis for batch-processes has been briefly illustrated, it can be applied to the CaL-CSP integration plant. In fact, the CaL process is clearly a time-dependent process since the operation of the calcination reactor is closely linked to the presence of solar radiation. First of all, the period corresponding to a 24-hour day was chosen as the batch cycle, i.e. the duration in which the calcium cycle for energy production in the CaL-CSP integration plant is repeated in the same way. As already mentioned, the calciner side works only during the daytime while the carbonator side runs 24 hours a day: assuming that solar radiation is captured in clear sky conditions, the duration of the daytime hours exploitable by the CSP application can be considered as 8 hours for the plant model under examination. Hence, the solar calciner is activated by solar radiation for 8 hours so it is supposed that the calcination process streams are available for the same time period. In contrast, the carbonation process streams are available for the entire 24-hour batch cycle. Furthermore, it can be assumed that all the streams involved in the CaL process are considered Type A streams in the classification just explained, greatly simplifying the pinch-analysis for the batch-process. On the basis of these considerations, it is reasonable to divide the batch cycle into two time intervals. In this way, the Time Events Diagram is constructed considering an 8-hour batch period

for the daylight hours and a 16-hour batch period for the nigh hours. The Fig. 22 shows the Time Event Diagram in which all the streams involved in the CaL process are reported according to each batch period.

Stream	***Type***	***Operating Time***	
		Start [h]	**End [h]**
1	CaO	8	16
2	Solids ($CaCO_3$+CaO)	8	16
3	CO_2 sensible	8	16
4	CO_2 compressed	8	16
5	CO_2 out, turbine	0	24
6	CO_2 out, compressor	0	24
7	CaO	0	24
8	Solids ($CaCO_3$+CaO)	0	24

Table 11. Stream identification for CaL-CSP application for pinch-analysis of batch-process.

As shown in Fig. 22, the time interval between 8h-16h contains the streams both of the calciner and carbonator side, while in the remaining time intervals only the process streams of the carbonation side are present.

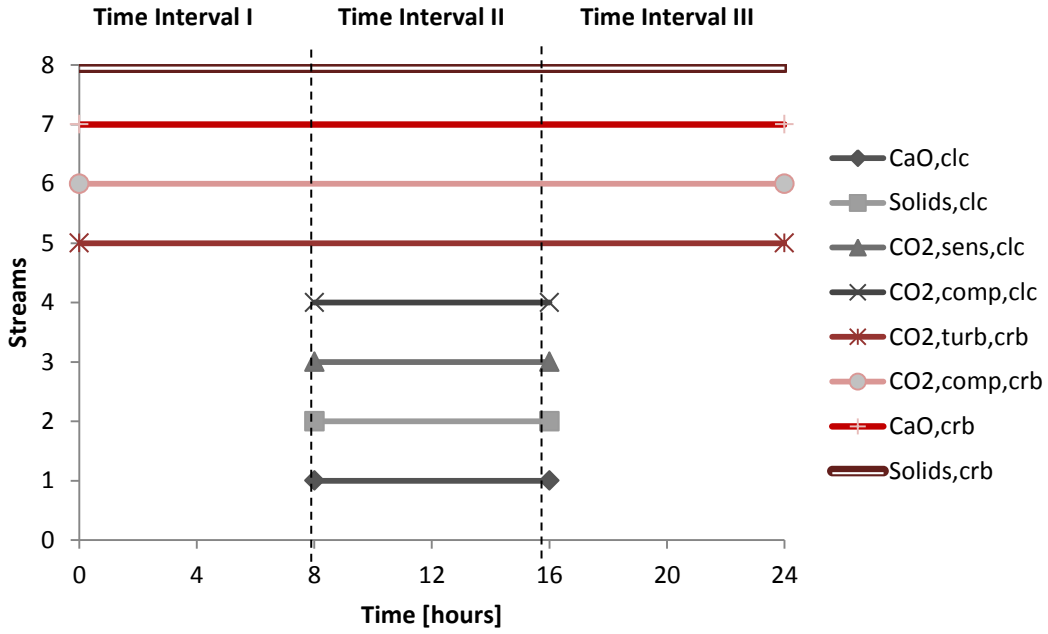

Figure 22. Time Event Diagram for pinch-analysis of the CaL-CSP plant considering the process streams both of calciner and carbonator side.

In order to evaluate the hot and cold utility targets of the batch-process, the heat cascade calculation is performed for each time interval. The two time intervals that correspond to the night hours between 0-8 and 16-24, as shown in the Time Interval Diagram, are merged in a single 16-hour time interval. The carbonator streams in the considered time interval are characterized both by the same supply and target temperatures and by the same heat capacity. Considering the data in Table. 4, the heat cascade in the second time interval results in the same pinch-analysis for the carbonator side reported in the previous section. In fact, the heat exchanger network allows to perform heat recovery in the same ways since the maximum and minimum heating and cooling requirements are unchanged. In the pinch-analysis for the batch period between 8-16 hours, a different heat exchanger configuration is obtained as the streams involved are different. Assuming that the minimum approach temperature for pinch-analysis is always 20°C, the Grand Composite Curve shows that the pinch-point temperature is equal to 426 °C for the hot streams and 406 °C for the cold streams. The maximum and minimum requirements for heating and cooling for the batch-period considered are shown in the Fig. 23. Since the streams present in the time interval under examination are the same as those assessed in the pinch-analysis of the continuous process, the maximum requirements for cooling and heating are the same.

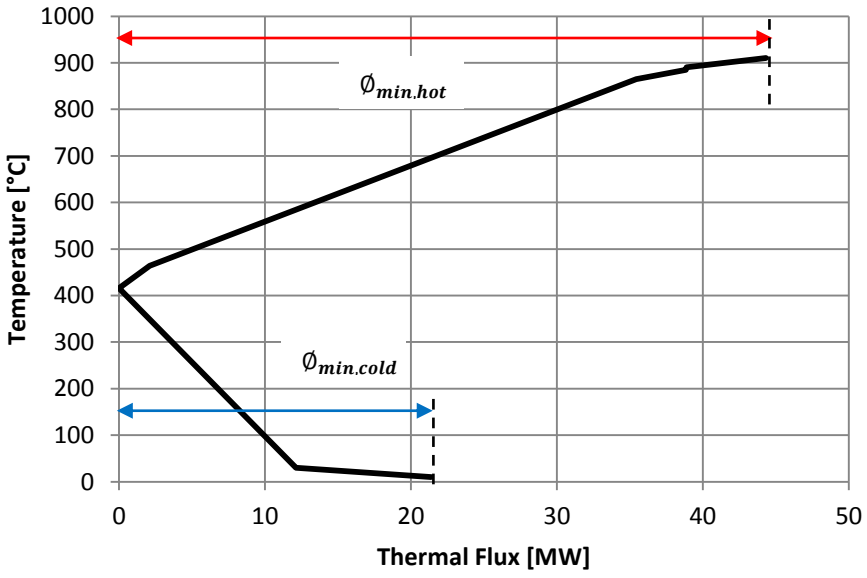

Figure 23. Grand Composite Curve for the streams considered in the pinch-analysis for the batch-process in the time interval between 8h-16h.

As reported in the Table. 12, the comparison of the minimum requirements for heating and cooling between the continuous and the batch process shows a slight difference

indicating that the heat exchanger network designed for the batch-process presents the same characteristics as the continuous process from the heat recovery point of view.

Type of Process	*Minimum Cooling requirements [MW]*	*Minimum Heating requirements[MW]*
Continuous	22,80	45,73
Batch (8h-16h)	21,39	44,32

Table 12. Comparison between the minimum requirements for cooling and heating in the continuous and batch processes.

The main difference of the heat exchangers network designed for the continuous process compared to the batch-process is the chance of coupling different process fluids. The thermal capacity and the supply and target temperatures of the streams included in the batch period are summarized in the Table. 3 and Table. 4. For completeness, the heat exchangers network for the batch-process in the time interval between 8h-16h is reported below in order to analyze the different configuration with respect to the continuous process.

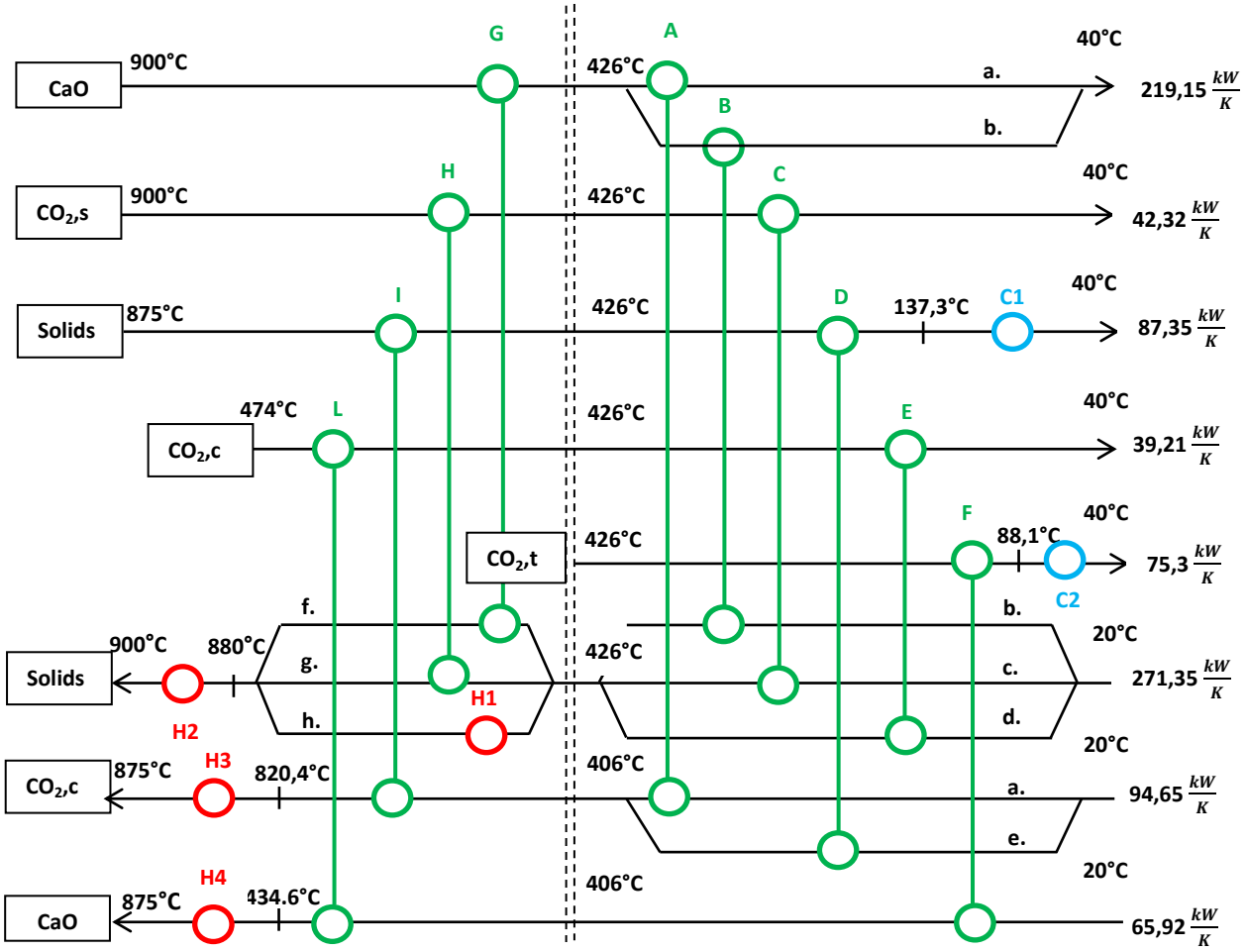

Configuration 1 – Base case

The heat capacities of the splitted streams summarized in the Table.13 allow to create the heat exchangers network shown above.

Above pinch-point		*Below pinch-point*	
Splitted streams	***Gc_p[kW/K]***	***Splitted streams***	***Gc_p[kW/K]***
f.	219,15	**a.**	29,32
g.	42,32	**b.**	189,83
h.	9,88	**c.**	42,32
		d.	39,21
		e.	65,33

Table 13. The heat capacity of the streams branches for the pinch-analysis of the batch-period between 8h-16h for the design of the heat exchangers network.

The thermal powers of each heat exchanger can be calculated by applying the equation used for the pinch-analysis of the continuous process. The results are summarized in the table below.

HEX	***Gc_p[kW/K]***	***Tin [°C]***	***Tout [°C]***	***Thermal power [MW]***
A	29,33	426	40	**11,32**
B	189,83	426	40	**73,27**
C	42,32	426	40	**16,33**
D	87,35	426	137,3	**25,22**
E	39,21	426	40	**15,14**
F	75,3	426	40	**25,45**
G	219,15	900	426	**103,88**
H	42,32	900	426	**20,07**
I	87,35	875	426	**39,22**
L	39,21	474	426	**1,88**
Cooler 1	87,35	137,3	40	**8,50**
Cooler 2	75,30	88,1	40	**3,62**
Heater 1	9,88	880	406	**4,49**
Heater 2	271,35	900	880	**5,43**
Heater 3	94.65	875	820,4	**5,17**
Heater 4	65.92	875	434,6	**29,66**

Table 14. Thermal powers of the heat exchangers, coolers and heaters for the configuration obtaioned for batch-period between 8h-16h.

The configuration of the heat exchangers network for the continuous process presents five heat exchangers both on the calciner and on the carbonator side. Therefore, the overall number of heat exchangers for the first configuration proposed is equal to the number of the second configuration for the batch-process. The same considerations are valid for the number of both coolers and heaters for the two configurations. The substantial difference lies in the fact of using hot streams of the calcination system to heat up those of the carbonator system and vice versa, making the two systems no longer independent.

However, the *Configuration 1* proposed for the heat exchangers network does not bring improvements compared to the first one, at least from the point of view of the heat recovery. Since the configuration under consideration does not allow to improve the performance of the CaL-CSP integration system, the operation in night mode is not analysed. In order to evaluate any enhancement from the engineering point of view of the system, the *Configuration 1* represents the base case through which the subsequent improved configurations will be compared with regard to the heat recovery options, the areas and the types of heat exchangers adopted in the proposed network configurations.

3.3.2 Optimized heat exchangers configuration for batch-process

The identification of the process streams in the batch-cycle for the pinch-analysis actually allows to study a further configuration of the heat exchangers network in order to improve the heat recovery and facilitate the system operation during day and night hours. As can be noticed in the Time Even Diagram, in the batch period between 8h-16h the same process streams that are first cooled then are re-heated: for example, the CaO stream that leaves the solar calciner at the calcination temperature is normally sent to the storage system after being cooled, then the cold CaO stream must be heated up to the carbonation temperature before entering the carbonator. The same considerations apply to both the $CaCO_3$ and CO_2 streams. Therefore in the event that calcination and carbonation systems no longer operate independently of each other, it is possible to evaluate a different configuration of the CaL-CSP integration system by identifying which streams of the calcination system are directly usable by the carbonator system and vice versa. From the analysis of the supply and target temperatures of the process streams, the CaO and CO_2 streams exiting the solar calciner can be conveyed directly to the carbonator in order to participate in the carbonation reaction, thus by-passing the

thermal storage. Similarly, the $CaCO_3$ stream produced by the carbonation reaction can be straight introduced into the calciner in order to carry out the calcination reaction. The CaL-CSP plant scheme in the Fig. 24 shows both the portion of the CO_2 and CaO mass flow rates sent to the storage system and the ones sent to the carbonator, as well as the portion of the $CaCO_3$ mass flow rate conveyed to the storage system and the one sent to the solar calciner. Furthermore, the proposed scheme in Fig. 24 is valid for the daytime operation of the CaL-CSP integration systems.

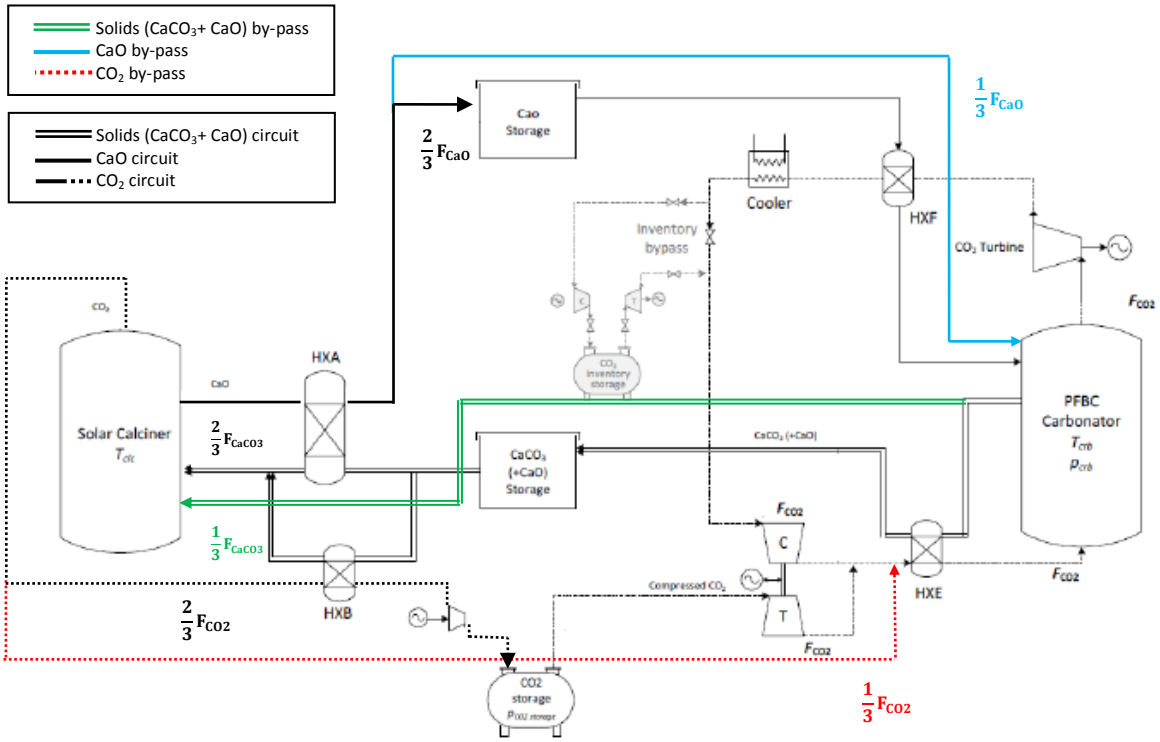

Figure 24. CaL-CSP scheme of the by-pass flows for the daytime operation and of the flows sent to the respective storage systems of CaO, CO_2 and $CaCO_3$ used to perform the pinch-analysis for the batch period between 8h-16h .

As previously explained, to perform the pinch-analysis it is necessary to identify which flows are involved in the batch process, their mass flow rates and the supply and target temperatures. Considering each available stream, it can be obtained:

- The hot CaO stream leaving the solar calciner at the calcination temperature of 900 °C is splitted into two streams whose mass flow rates are calculated by means of the mass balance equation. The CaO mass flow rate required to drive the carbonation reaction is equal to one third of the CaO flow rate produced by the calcination reaction as shown in the equation:

$$(\overline{F_{CaO,crb}})_{by-pass} = \frac{1}{3} \cdot \overline{F_{CaO,clc}}$$

In general, the streams entering the carbonator must be brought to the carbonation temperature of 875 °C, which therefore corresponds to the target temperature of the by-pass CaO stream. The remaining fraction of the CaO stream leaving the calcination reactor equal to $\frac{2}{3} \cdot \overline{F_{CaO,clc}}$ is sent to the CaO storage system reaching the ambient temperature of 20 °C

- The hot CO_2 stream exiting the solar calciner at 900 °C is also separated into two streams whose mass flow rates are calculated in the same way as in the previous case so the by-pass CO_2 stream is written below

$$(\overline{F_{CO2,crb}})_{by-pass} = \frac{1}{3} \cdot \overline{F_{CO2,clc}}$$

and sent directly to the carbonation reactor. The target temperature is always equal to 875 °C. In contrast, the CO_2 stream fraction equal to $\frac{2}{3} \cdot \overline{\boldsymbol{F_{CO2,clc}}}$ is cooled down to the ambient temperature of 20 °C. After compression, the temperature of the CO_2 stream reaches 474 ° C and before being conveyed to the storage system it must be cooled down again to ambient temperature

- In the carbonator side, the hot CO_2 stream leaving the carbonation reactor is sent to the gas turbine in order to extract the mechanical power to be converted into electrical power. The outlet temperature of the gas turbine is equal to 426 ° C, i.e. the temperature at which the CO_2 stream is available for the heat exchange. The target temperature is always equal to the ambient temperature
- The hot $CaCO_3$ stream exits the carbonator at the temperature of 875 °C and is sent directly to the solar calciner, maintaining its mass flow rate. However, the mass flow rate of the $CaCO_3$ required to drive the calcination reaction is three times greater than the one produced by the carbonator according to the mass balance equation. So in addition to the CaCO3 mass flow rate from the carbonator system, a fraction of $CaCO_3$ extracted from its storage system is required to carry out the calcination reaction. The storage temperature at which $CaCO_3$ is found is 20 °C and before entering the solar calciner it must be preheated up to 900 °C.

On the basis of the considerations just presented, the results that express the mass flow rates of the process streams are summarized in the Table. 15. Furthermore, in order to determine the thermal capacity of each stream, the specific heat values are provided by the simulation tests carried out in the Alovisio work (3), in which the evaluation was performed considering different mathematical correlations based on both the different substances used in the CaL-CSP integration system and the extremes of each temperature range of the process streams.

Stream	***Type***	$\dot{m}$	$\bar{c}_p$	$G \cdot \bar{c}_p$
		$\frac{kg}{s}$	$\frac{kJ}{kg \cdot K}$	$\frac{kW}{K}$
$\frac{2}{3} \cdot \overline{F_{CaO,clc}}$	Hot	153	0.955	146.10
$\frac{1}{3} \cdot \overline{F_{CaO,clc}}$	Hot	76,5	0.955	73.05
$\frac{2}{3} \cdot \overline{F_{CO2,sens,clc}}$	Hot	24	1.175	28.21
$\frac{2}{3} \cdot \overline{F_{CO2,comp,clc}}$	Hot	24	1.089	26.14
$\frac{1}{3} \cdot \overline{F_{CO2,sens,clc}}$	Hot	12	1.175	14.11
$\frac{2}{3} \cdot \overline{F_{CaCO3,clc}}$	Cold	177	1.022	180.90
$\overline{F_{CO2,turb,crb}}$	Hot	73,8	1.020	75.30
$\overline{\overline{F_{CO2,comp,crb}}}$	Cold	73.8	1.103	81.41
$\overline{F_{CaCO3,crb}}$	Cold	88.5	0.987	87.35

Table 15. Results of the calculation of the mass flow rates for the pinch-analysis in the batch period between 8h-16h in order to build the optimized configuration of the heat exchangers network.

The identification of the streams must be completed by identifying the supply and target temperatures in order to proceed with the pinch-analysis. The data are reported in the following table.

Stream	*Type*	$G \cdot \bar{c}_p \left[\frac{kg}{s}\right]$	$T_s[°C]$	$T_t[°C]$
$\frac{2}{3} \cdot \overline{F_{CaO,clc}}$	Hot	146.10	900	20
$\frac{1}{3} \cdot \overline{F_{CaO,clc}}$	Hot	73.05	900	875
$\frac{2}{3} \cdot \overline{F_{CO2,sens,clc}}$	Hot	28.21	900	20
$\frac{2}{3} \cdot \overline{F_{CO2,comp,clc}}$	Hot	26.14	474	20
$\frac{1}{3} \cdot \overline{F_{CO2,sens,clc}}$	Hot	14.11	900	875
$\frac{2}{3} \cdot \overline{F_{CaCO3,clc}}$	Cold	180.90	20	900
$\overline{F_{CO2,turb,crb}}$	Hot	75.30	426	20
$\overline{F_{CO2,comp,crb}}$	Cold	81.41	20	875
$\overline{F_{CaCO3,crb}}$	Cold	87.35	875	900

Table 16. Stream identification for the pinch-analysis of the batch process for the optimized configuration of the heat exchanger network.

The minimum temperature approach ΔT_{min} for the pinch-analysis is set at 20°C. In order to find the minimum requirements for heating and cooling, it is necessary to build the Heat Cascade as explained in the previous section. The results for the batch-period between 8h-16h are summarized in the Table. 17.

$T_{shifted}$	$\sum_{i}^{n,hot} (Gc_p)_i - \sum_{i}^{n,cold} (Gc_p)_i$	*Thermal flux*	*Infeasible Heat Cascade*	*Feasible Heat cascade*
°C	*kW/K*	*kW*	*kW*	*kW*
910	0	0	0	**43674**
890	-268,25	-5365	-5365	**38309**
885	-6,79	-34	-5399	**38275**
865	-0,85	-17	-5416	**38258**
464	-88,00	-35289	-40705	**2969**
416	-61,86	-2969	-43674	**0**
30	13,44	5187	-38487	**5187**
10	275,75	5515	-32972	**10702**

Table 17. Analytical method for pinch-analysis in order to identifying the minimum requirements of heating and cooling through the feasible heat cascade.

The shifted pinch-point temperature is 416°C, therefore the pinch-point temperature for hot streams is 426 °C while for cold streams is 406 °C. In the Fig. 25 is shown the Grand Composite Curve of the optimized case with respect to base case.

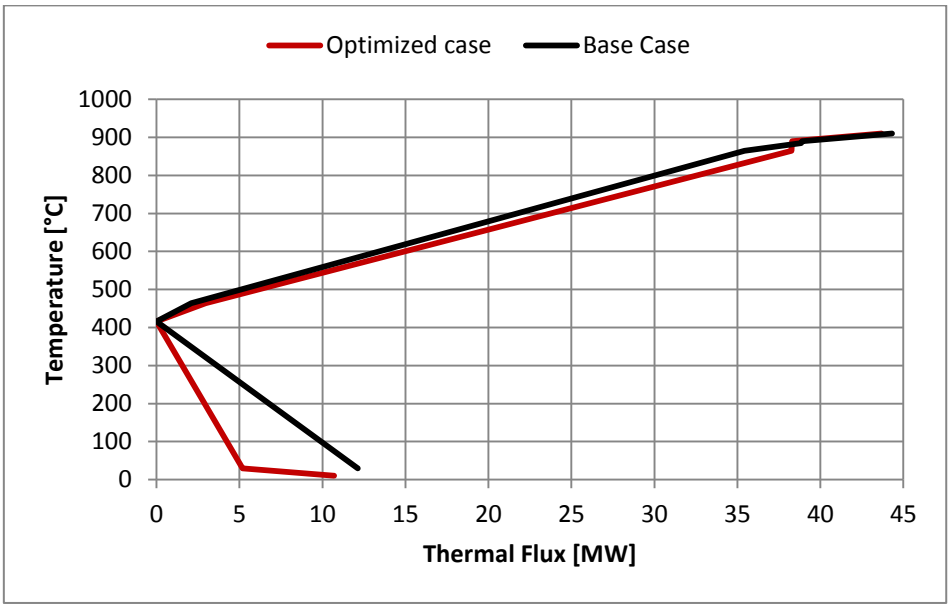

Figure 25. comparison between the grand composite curves generated for the base case and for the optimized case

The Table. 18 shows the minimum requirements for cooling and heating analysed previously for the continuous process pinch-analysis and for the batch-process *Configuration 1* in order to compare the results with batch-process *Configuration 2.* The minimum requirements for heating show a slight decrease, while those for cooling are basically halved.

Type of Process	***Minimum Cooling requirements [MW]***	***Minimum Heating requirements [MW]***
Continuous	22,80	45,73
***Configuration 1*-Batch (8h-16h)**	21,39	44,32
***Configuration 2*-Batch (8h-16h)**	10,70	43,67

Table 18. Comparison of the minimum requirements for heating and cooling for different configuration analysed.

The *Configuration 2* allows a performance improvement from the heat recovery point of view compared to the other ones investigated. As mentioned above, it is necessary to consider that part of the external heat requirement of the fluids that are part of the carbonator system is satisfied by the carbonation heat.

Given the results obtained, the *Configuration 2* of the heat exchangers network has been designed based on the practical rules of pinch-analysis listed in the section above.

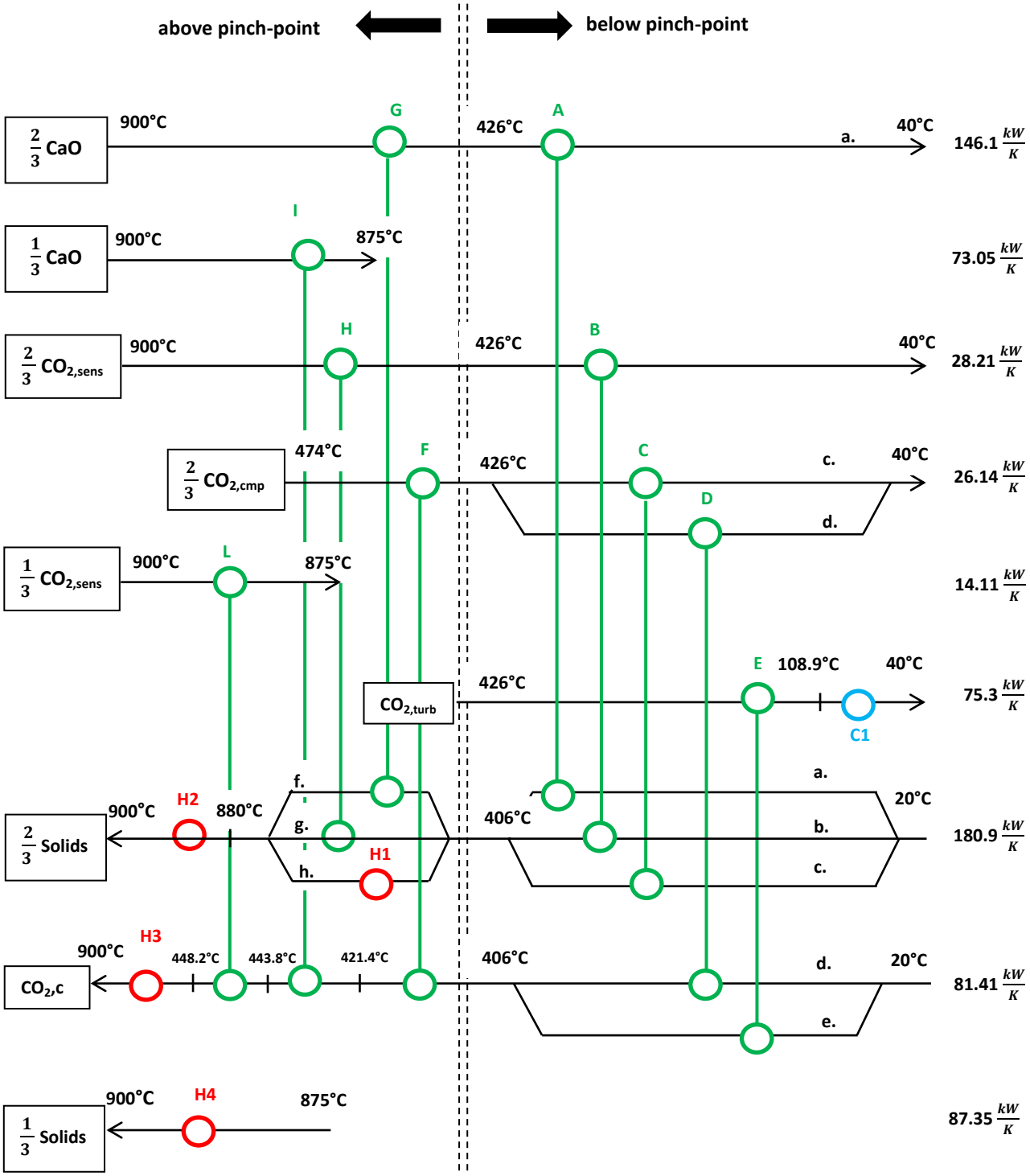

Configuration 2

The splitted streams for the heat exchanger network designed in the *Configuration 2* are shown in the table below.

Above pinch-point		*Below pinch-point*	
Splitted streams	***Gc_p[kW/K]***	***Splitted streams***	***Gc_p[kW/K]***
f.	146.1	**a.**	146.1
g.	28.21	**b.**	28.21
h.	6.59	**c.**	6.59
		d.	19.55
		e.	61.86

Table 19. Splitted streams for the heat exchanger network analysed in the Configuration 2.

The thermal powers of each heat exchanger used in the network under consideration are reported in the following table.

HEX	***Gc_p[kW/K]***	***Tin [°C]***	***Tout [°C]***	***Thermal power [MW]***
A	146.1	426	40	**56.39**
B	28.21	426	40	**10.89**
C	6.59	426	40	**2.54**
D	19.55	426	40	**7.55**
E	75.30	426	108.9	**23.88**
F	146.1	900	426	**69.25**
G	28.21	900	426	**13.37**
H	26.14	474	426	**1.25**
I	73.05	900	875	**1.83**
L	14.11	900	875	**0.35**
Cooler 1	75.30	108.9	40	**5.19**
Heater 1	180.9	900	880	**3.62**
Heater 2	6.59	880	406	**3.12**
Heater 3	81.41	875	448.2	**34.75**
Heater 4	87.35	900	875	**2.18**

Table 20. Heat exchangers thermal power for the Configuration 2

A quantitative analysis between the thermal powers of the *Configuration 1* and the *Configuration 2* shows a substantial reduction of the values mainly due to the reduction in the mass flow rates of the process streams available for the heat exchanger, as reported in the previous discussion. The number of heat exchangers below and above

the pinch-point for the *Configuration 2* is equal to ten, as well as for *Configuration 1*, but with lower thermal powers, a reduction in the heat exchange areas is expected in order to achieve the aim of this study.

In general, to verify the feasibility of building a network of heat exchangers as designed in the various proposed configurations, it is necessary to evaluate whether the correct operation of the system is also guaranteed in night mode. In fact, the network design of the heat exchangers must take into account that the flows related to the calcination system will not be present in the absence of solar radiation. The following figure shows a system scheme in which the flows involved during the night are identified (Fig. 26).

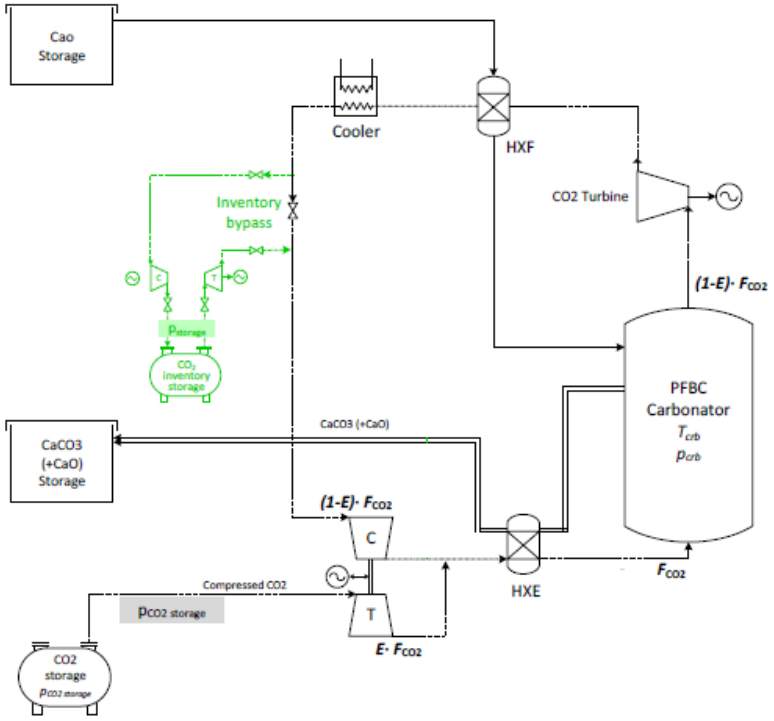

Figure 26. Process streams of the carbonator side system operating in the nigh mode **(3)**.

With reference to *Configuration 2*, in the night batch period the process fluids that would still be present are those relating to CO_2. On the other hand, CaO and $CaCO_3$ streams would become available for heat exchange according to the same methods analyzed in the carbonator side configuration. The heat exchangers below the pinch-point D and E of the *Configuration 2* would remain active during the night, since they are fed by the CO_2 streams. By comparing these two heat exchangers with those present in the carbonator side configuration involving the same CO_2 streams, it is noted that the thermal powers and thermal capacities are not comparable. In addition, the CO_2 stream

leaving the gas turbine is divided into two streams in the carbonator side configuration as opposed to *Configuration 2*, as well as the thermal capacities of the CO_2 splitted streams extracted from the CO_2 storage have values that are not comparable. For this reason, a third configuration has been studied in such a way as to allow the network of heat exchangers to operate even during the night, trying to maintain the same the CO_2 splitted streams.

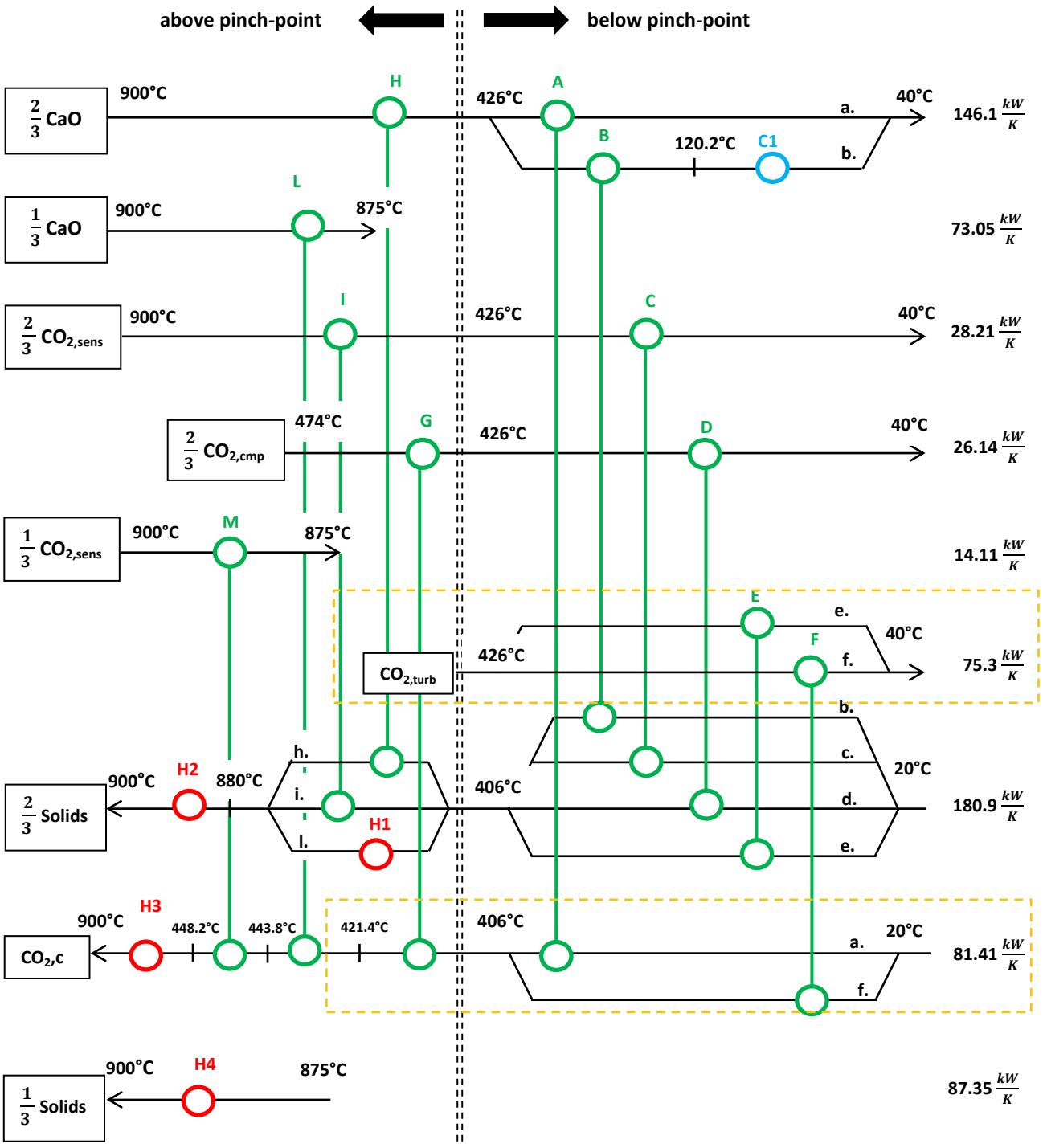

Configuration 3 – Optimized case

The splitted streams for the heat exchanger network of *Configuration 3* are summarized in the Table. 21.

Above pinch-point		*Below pinch-point*	
Splitted streams	***Gc_p[kW/K]***	***Splitted streams***	***Gc_p[kW/K]***
g.	146,1	**a.**	72,03
h.	28,21	**b.**	74,07
i.	6,59	**c.**	28,21
		d.	12,70
		e.	65,92
		f.	9,38

Table 21. Splitted streams of the heat exchangers network in the Configuration 3.

As for the previous configurations analysed, the thermal powers of the heat exchangers present in *Configuration 3* are shown in the Table. 22. The heat exchangers in *Configuration 3* are eleven, i.e. one more than in *Configuration 2.*

HEX	***Gc_p[kW/K]***	***Tin [°C]***	***Tout [°C]***	***Thermal power [MW]***
A	72,03	426	40	**27,80**
B	74,07	426	40	**28,59**
C	28,21	426	40	**10,89**
D	26,14	426	238,5	**4,9**
E	65,92	426	40	**25,45**
F	9,38	426	40	**3,62**
G	146,1	474	426	**1,25**
H	28,21	900	426	**65,25**
I	26,14	900	426	**13,37**
L	73,05	900	875	**1,83**
M	14,11	900	875	**0,35**
Cooler 1	26,14	238,5	40	**5,19**
Heater 1	180,9	900	880	**3,62**
Heater 2	6,59	880	406	**3,12**
Heater 3	81,41	875	448,2	**34,75**
Heater 4	87,35	900	875	**2,18**

Table 22. Thermal power of the heat exchangers in the Configuration 3.

The CO_2 streams identified by the dashed lines in *Configuration 3* are comparable with those present in the carbonator side configuration. The detailed analysis of the individual heat exchangers allows to highlight that:

- The heat exchanger E of the *Configuration 3* is similar to the heat exchanger A of the carbonator side configuration as regards the type of heat exchanger (gas-solid), the temperature range and consequently the thermal powers (data found in the Table. 10 and Table. 22)

Configuration 3					
HEX	**Type**	***Gc_p[kW/K]***	***Tin [°C]***	***Tout [°C]***	***Φ[MW]***
E	**$CO_{2,turb}$(hot)**	65,92	426	40	**25,45**
	Solids (cold)	65,92	20	406	
Configuration-Carbonator side					
HEX	**Type**	***Gc_p[kW/K]***	***Tin [°C]***	***Tout [°C]***	***Φ[MW]***
A	**$CO_{2,turb}$(hot)**	65,92	426	40	**25,45**
	CaO (cold)	65,92	20	406	

In the daily mode, the streams connected by the heat exchanger E are the $CO_{2,turb}$ leaving the turbine (carbonator) and the solid stream of $CaCO_3$+CaO (calciner). During the night the $CaCO_3$+CaO solid stream no longer exists, so the $CO_{2,turb}$ can perform the heat exchange with CaO solid stream (carbonator) respecting the Logarithmic Mean Temperature Difference (LMTD), thus operating as the heat exchanger A

- The heat exchanger F of the *Configuration 3* is identical to the heat exchanger B of the carbonator side configuration and moreover the streams involved in the heat exchange are present continuously in the batch cycle

Configuration 3					
HEX	**Type**	***Gc_p[kW/K]***	***Tin [°C]***	***Tout [°C]***	***Φ[MW]***
F	**$CO_{2,turb}$(hot)**	9,38	426	40	**3,62**
	$CO_{2,comp}$ (cold)	9,38	20	406	
Configuration-Carbonator side					
HEX	**Type**	***Gc_p[kW/K]***	***Tin [°C]***	***Tout [°C]***	***Φ[MW]***
B	**$CO_{2,turb}$(hot)**	9,38	426	40	**3,62**
	$CO_{2,comp}$ (cold)	9,38	20	406	

- The heat exchanger A of the *Configuration 3* is comparable to the heat exchanger C of the carbonator side configuration about the type of heat exchanger (gas-solid) and despite the different temperature range as well as the thermal powers (data found in the Table. 10 and Table. 22)

Configuration 3					
HEX	**Type**	Gc_p***[kW/K]***	***Tin [°C]***	***Tout [°C]***	***Φ[MW]***
A	**CaO (hot)**	72,03	426	40	**27,80**
	$CO_{2,comp}$ (cold)	72,03	20	406	
Configuration-Carbonator side					
HEX	**Type**	Gc_p***[kW/K]***	***Tin [°C]***	***Tout [°C]***	***Φ[MW]***
C	**Solids (hot)**	87,35	426	49,2	**32,91**
	$CO_{2,comp}$ (cold)	85,27	20	406	

In the daily mode, the streams connected by the heat exchanger A are the CaO stream (calciner) and the $CO_{2,comp}$ stream (carbonator). In the night mode the CaO solid stream stops flowing, so the $CO_{2,comp}$ can perform the heat exchange with the $CaCO_3$+CaO solid stream (carbonator). In this case, it is necessary to size the heat exchanger on the basis of the maximum thermal power between the two exchanger considered, i.e. the heat exchanger C, so that it can work in both modes and with both combinations of streams.

Above the pinch-point, *Configuration 3* requires different considerations since it has a single fluid which is part of the carbonator system (the cold $CO_{2,comp}$ stream). In fact, it is necessary to evaluate which heat exchangers of the *Configuration 3* can be used by the carbonator streams that appear during the night mode (the hot $CaCO_3$+CaO solid stream and the cold CaO solid stream). The heat exchangers analysis results in:

- The heat exchanger E in the carbonator side configuration involves the hot $CaCO_3$+CaO solid stream and the cold CaO solid stream as reported in the table below

Configuration-Carbonator side					
HEX	**Type**	Gc_p***[kW/K]***	***Tin [°C]***	***Tout [°C]***	***Φ[MW]***
E	**Solids (hot)**	65,92	875	426	**29,60**
	CaO (cold)	85,27	406	855	

Based on the thermal power of the heat exchanger E, the only heat exchanger that could be used among the ones in the *Configuration 3* is the heat exchanger H as it has a higher thermal power, the same LMTD and the same type of coupled streams (solid-solid). For completeness, the characteristics of the heat exchanger H are shown in the table below.

Configuration 3					
HEX	**Type**	Gc_p***[kW/K]***	***Tin [°C]***	***Tout [°C]***	***Φ[MW]***
H	**CaO (hot)**	146,1	900	426	**65,25**
	Solids (cold)	146,1	880	406	

- The heat exchanger D in the carbonator side configuration couples the hot $CaCO_3$+CaO solid stream and the cold $CO_{2,comp}$ stream as reported in the table below

Configuration-Carbonator side					
HEX	**Type**	Gc_p***[kW/K]***	***Tin [°C]***	***Tout [°C]***	***Φ[MW]***
D	**Solids (hot)**	21,43	875	426	**9,62**
	$CO_{2,comp}$ (cold)	94,65	507,7	406	

Based on the type of streams coupled in the heat exchanger (gas-solid), the only heat exchanger that could be used among the ones in the *Configuration 3* is the heat exchanger L since it involves the CaO solid stream and the $CO_{2,comp}$ stream despite the lower thermal power and the different LMTD. Then, the heat exchanger D can operate both in the daily and night modes. The features of the heat exchanger L are shown in the table below.

Configuration 3					
HEX	**Type**	Gc_p***[kW/K]***	***Tin [°C]***	***Tout [°C]***	***Φ[MW]***
L	**CaO (hot)**	73,05	900	875	**1,83**
	$CO_{2,comp}$ (cold)	146,1	443,8	421,4	

In order to verify the validity of the considerations just mentioned, it is necessary to calculate the area of the heat exchanger to assess whether they are able to operate in both night and day mode. The heat exchange areas will be assessed in the next section as it represents a necessary parameter also for the economic analysis.

Chapter IV

Economic analysis for heat exchangers network

In general, the economic analysis is performed in order to assess whether the technological improvements studied for a given system are able to guarantee an economic advantage as well. In particular in the energy sector, technological advances in applications are often accompanied by an unaffordable economic expenditure which limits its competitiveness and its commercial expansion in the energy market. Therefore, this section is dedicated to the economic analysis of the heat exchanger networks designed for the CaL-CSP integration of the SOCRATCES project to evaluate whether the design improvements analysed in the previous sections are cost-effective.

The economic analysis approach chosen for this project was developed by the National Energy Technology Laboratory (NETL) of the United States Department of Energy (DOE). In fact, the cost estimation methodology proposed by NETL allows to determine not only the capital cost for power production systems, but also the cost metrics, or a set of indicators aimed at predicting the trend of the main cost variables with which different technological systems are compared (11).

4.1 Capital Cost assessment

The cost assessment methodology involves five different levels of capital costs, that are the fixed initial investments costs necessary for the construction of the new power production systems:

- The Bare Erected Cost (BEC) includes the costs of process equipment, on-site facilities and infrastructure to support the system, direct and indirect labor for construction and installation. BEC is an “overnight” cost expressed in the “base-year” dollars, i.e. the first year of capital expenditure (12)

- The Engineering, Procurement and Construction Cost (EPCC) includes the BEC with in addition the costs of services supplied by engineering, procurement and construction contractor, such as detailed design, contractor permitting, project and construction management **(12)**. EPCC is also an overnight cost expressed in the base-year dollars
- The Total Plant Cost (TPC) includes the EPCC plus the project and process contingencies. TPC is an overnight cost always expressed in the base-year dollars
- The Total Overnight Capital (TOC) includes the TPC with in addition the all overnight costs, such as pre-production, inventory capital, financing and other owner's costs **(12)**. TOC is an overnight cost expressed in the base-year dollars
- The Total As Spent Capital (TASC) includes the TOC and all the escalation and interest of debt during the capital expenditures period. Therefore, TASC is expressed in mixed-current-year dollars over the capital expenditure period.

Based on the numerous techno-economic studies conducted by NETL, the result obtained through the cost estimation methodology presents an expected accuracy that varies between -15% and + 30% compared to the real value (12).

Project definition	**Typical Engineering Completed**	**Expected accuracy**
1 to 15%	- plant capacity, block schematics, indicated layout, process flow diagrams for main process - systems, and preliminary engineered process and utility - equipment lists	-15% to -30% on the low side, and +20% to +50% on the high side

Table 23. Features of a cost estimate for a "Feasibility study" of a generic power plant **(12)**.

Therefore, the cost estimate through the methodology developed by NETL shows a not negligible inaccuracy with respect to the real value. The cost estimation in this manuscript is performed to identify which configuration of the heat exchangers network is more advantageous both from an economic and plant engineering point of view, then the accuracy is assumed to be the same for each scenario analyzed. Furthermore, since the configurations of the CaL-CSP integration system differ only in the network of heat exchangers, the economic analysis is performed only for this part of the plant design.

The calculation methods used for the estimation of the capital costs are presented in the following sections for each component of the heat exchanger network.

4.1.1 BEC estimation

The BEC estimation for a production system is based on the calculation of the initial investment costs of each plant component. The NETL cost estimation methodology foresees the use of polynomial cost functions obtained experimentally through a rather large database of the capital costs for different thermal components. The cost functions for each system equipment are able to express the cost in basic conditions as a function of the main operating parameters of the components under the form of multiplying factors. In particular, the main component on which the economic analysis of this work is concerned is the heat exchanger.

Based on the different types of heat exchanger, there are two distinct cost functions shown below:

- the cost function for the gas-gas exchange, for the cooling stage (air cooling), for heating stage (gas-gas exchange between cold streams and flue gases exiting a combustion chamber) and for combustion chamber is expressed as **(13)**:

$$C_{BEC} = C_P^0 \cdot (B_1 + B_2 \cdot F_M \cdot F_P)$$

where

- C_P^0 is the purchasing cost of the is the purchasing cost of equipment referred to base conditions (e.g. common material, ambient conditions)
- B_1 and B_2 are constant parameters correlated to the type of equipment
- F_M is the material factor, which is mainly affected by the operating temperature
- F_P is the pressure factor, which depends on the operating pressure.

The purchasing cost C_P^0 of the component is in turn expressed by means of a logarithmic function as:

$$log_{10}C_P^0 = K_1 + K_2 \cdot log_{10}\mathrm{A} + K_3 \cdot (log_{10}\mathrm{A})^2$$

where

- K_1, K_2 and K_3 are constants which depend on the type of equipment
- A is the size parameter expressed in (m^2) for heat exchangers

The K_1, K_2, K_3 and A values are summarized in Table. 24 considering the experimental data found in (13) for different type of equipment.

Type of exchange	Model	K_1	K_2	K_3	Minimum A of validity	Maximum A of validity
Gas-gas, heating stage	Shell and tube	4.184	-0.2503	0.1974	10	1000
Cooling stage	Air cooler	4.0336	0.2341	0.0497	10	10000

Table 24. Values of K_1, K_2, K_3 for the purchasing cost evaluation of heat exchangers.

The size parameter A of the heat exchanger is determined by means of the formula in which the heat flux exchanged between the two streams of the heat exchanger is divided by the Logarithmic Mean Temperature Differences (LMTDs) and the Global Heat Transfer coefficient U appear:

$$A = \frac{\emptyset}{\Delta T_{ml} \cdot U}$$

On the basis of the type of exchange, the ΔT_{ml} is assessed differently in order to consider the non-linear trend of the temperature within the heat exchanger:

- For gas-gas exchange and heating stage, the value of the Logarithmic Mean Temperature Differences (LMTDs) is calculated as:

$$\Delta T_{ml} = \frac{\Delta T_1 - \Delta T_2}{ln\left(\frac{\Delta T_1}{\Delta T_2}\right)}$$

where the ΔT_1 and ΔT_2 are the temperature difference respectively in the section 1 and in the section 2 of a heat exchanger between counter-current hot and cold fluids

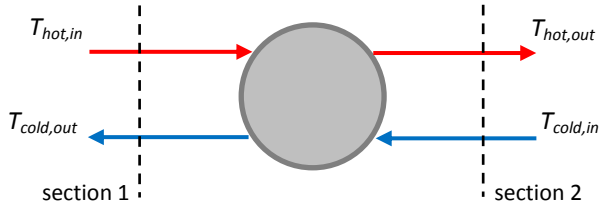

- For heating stage, the LMTD evaluation depends on the number of stages in which the heat exchange occurs. In the case of a single heating stage, the heat exchange between hot and cold flows occurs considering the supply temperature of the hot flow equal to the adiabatic flame temperature while the target temperature of the hot flow is set at 15°C higher with respect to the inlet temperature of the cold flow

- For cooling stage, the LMTD is set equal to 15°C for single cooling stage.

The values of the Global Heat Transfer coefficient U assumed for the gas-gas exchange for different for different process fluids (CO_2 and air) are summarized in the Table. 25 and taken from the scientific literature (14) (15).

Type of exchange	$\boldsymbol{U\left[\frac{W}{m^2K}\right]}$
CO_2-gas	100
Air-gas	35

*Table 25. Global Heat Transfer coefficient **U** for gas-gas heat exchangers.*

In the event that the value of A is out of of the validity range, it must be rescaled with the following expression:

$$C_1 = C_0 \left(\frac{S_1}{S_0}\right)^{0.6}$$

where C_0 are the cost evaluated with the cost function reported above with the size parameter S_0 equal to the nearest limit value, while S_1 is the size parameter of the real component.

The size parameter of the combustion chamber is actually the volume V (m^3), therefore different values K_1, K_2 and K_3 must be taken into consideration. Then, the volume of the combustion chamber is calculated assuming the mean volume flow rate between the inlet and outlet section of the component and multiplying it by a residence time of 0.5 s.

Type of exchange	**Model**	$\boldsymbol{K_1}$	$\boldsymbol{K_2}$	$\boldsymbol{K_3}$	**Minimum V of validity**	**Maximum V of validity**
Combustion chamber	Horizontal	3.5565	0.3776	0.0905	0.1	628

Table 26. Values of $\boldsymbol{K_1}$, $\boldsymbol{K_2}$, $\boldsymbol{K_3}$ for the purchasing cost evaluation for combustion chambers.

The material factor F_M in this economic analysis can assume three different values based on the operating temperature of the heat exchange:

- $F_M = 1$ for heat exchangers below the pinch-point built using the carbon steel
- $F_M = 2.75$ for heat exchangers above the pinch-point since the use of stainless steel guarantees better performance at high temperatures

- $F_M = 7.1$ for the combustion chamber built using a nickel alloy because the operating temperature are even higher.

The pressure factor F_P, as well as the purchasing costs, can be evaluated though a logarithmic function expressed as follows:

- $F_P = 1$ when the operating pressure is equal to 1 bar and it is the case in which the heat exchangers and combustion chambers fall
- Whereas the operating pressure of the component is higher than ambient one (1 bar), the F_P is evaluated using the logarithmic function expressed as follows:

$$log_{10}F_P = C_1 + C_2 \cdot log_{10}P + C_3 \cdot (log_{10}P)^2$$

where C_1, C_2, and C_3 are constant parameters which depend on type of component under investigation and P is the operating pressure of the component. These consideration are valid for gas-gas exchange and heating stage. In the Table. 27 are summarized the data used for the $F_P$evaluation.

Type of exchange	Model	C_1	C_2	C_3	Minimum P of validity	Maximum P of validity
Gas-gas, heating stage	Shell and tube	-0.00164	-0.00627	0.0123	5	140

Table 27. Values of C_1, C_2, and $C_3$for factor pressure evaluation.

Finally, the values of the B_1 and B_2 parameters are obtained experimentally according to the type of components and are summarized in the Table. 28.

Type of equipment	B_1	B_2
Gas-gas, heating stage	1.63	1.66
Air cooling	0.96	1.24
Combustion chambers	1.49	1.52

Table 28. Values of B_1 and $B_2$for the C_{BEC}.

- The second cost function for gas-solid heat exchanger, in particular for shell-plate exchangers between solid particles and supercritical CO_2 at high temperatures is present in the Albrecht et al. **(16)** work and expressed as:

$$C_{BEC} = 18.4784 \cdot (UA)^{0.67} \cdot (P)^{0.28}$$

The experimental correlation can be used not only for gas-solid but also solid-solid heat exchangers since they consist as the latter consist of two gas-solid

exchangers indirectly connected by means of a proper heat transfer fluid. The pressure value P considered in the formula is assumed as the maximum between the pressure of the two streams of the heat exchanger, while the product (UA) is calculated as the ratio between the heat flow exchanged between the two streams involved in the heat exchange and the LMTD:

$$UA = \frac{\emptyset}{\Delta T_{ml}}$$

The LMTD for the gas-solid heat exchangers is evaluated using the same formula for gas-gas heat exchanger, whereas for the solid-solid heat exchanger it can easily be shown that the LMTD of two indirect gas-solid heat exchangers is equal to half the LMTD for a single gas-solid heat exchanger:

$$\Delta T_{ml,indirect,ex} = \frac{1}{2}\Delta T_{ml,direct,ex}$$

The result of the cost function is valid for the high operating temperatures of the equipment. In order to guarantee the validity of the cost function for heat exchangers operating at low temperatures it is necessary to introduce a corrective factor that takes into consideration the material of the component, such as the material factor F_M. Then, the cost function can be expressed as:

$$C_{BEC,low\,T} = \frac{1}{2.75} C_{BEC,high\,T}$$

The BEC of each component calculated with the cost functions refers to the value of a specific year. In fact, it is necessary to consider the effect of time on the components costs due to the different monetary value, inflation and escalation. Since the first cost function refers to 2001 and the second one to 2018, it is possible to carry over all costs to 2018 by applying the following formula to the BEC obtained for 2001:

$$\frac{C_{BEC,2018}}{C_{BEC,2001}} = \frac{I_{2018}}{I_{2001}}$$

where *I* is the cost index of a specific year, the values of which are taken from Chemical Engineering Plant Cost Index (CEPCI) and summarized in the Table. 29.

Year	CEPCI
2001	397
2018	603.1

Table 29. Values used for CEPCI **(17)**.

4.1.2 EPCC estimation

The management of the engineering, procurement and construction of a production system is generally entrusted to external companies and then to multiple contractors or subcontractors. This contractual strategy allows the owner to have greater control over the project and reduce most of the risk premiums associated with EPC contracts that must be paid to the secondary companies. In fact, the traditional lump-sum agreement for EPC provided for a single contracting company to take on all the performance, planning and costs risks, in exchange for a substantial economic support, thus resulting in a significant increase in the project costs (12).

According to the NETL cost estimation methodology, EPC contract services are estimated between 8% and 10% of the BEC in today's market.

4.1.3 TPC estimation

Process and project contingencies are included in the TPC estimation in order to take into account unexpected costs related to engineering and design uncertainties of the project. The costs of the process contingencies are connected to the state of the art of the technology: in fact, a less developed technology presents greater uncertainties of the performance and therefore higher costs than a more mature technology. The NETL methodology assesses the process contingencies for different types of plants considering the current state of technology. The data are summarized in Table. 30.

Technology status	**Process Contingency (% of Associated Process Capital)**
New concept with limited data	+40%
Concept with bench-scale data	30% - 70%
Small pilot plant data	20% - 35%
Full-sized modules have been operated	5% - 20%
Process is used commercially	0% - 10%

Table 30. Process contingencies according to technologies maturity **(12)**.

Although the economic analysis is conducted for heat exchangers and combustion chambers, the type of general process underlying the CaL-CSP integration plant is in an experimental phase such as to fall into the category of small pilot plants and the costs of the process contingencies are estimated at 30% of the EPCC.

On the other hand, the project contingencies costs are evaluated starting from the costs of the process contingencies to which 15% of EPCC is added.

4.1.4 TOC estimation

The TOCs estimate the owner's costs linked to the activities that precede the plant's operating phase and consist of (12):

- Pre-production costs which concern the additional costs due to the preliminary phase of the project in which the components are tested using labor, materials and fuels. The pre-production costs correspond to the 2% of the TPC
- Inventory capital mainly of fuel resources and consumables needed for the pre-production phase. Spare part costs are estimated at 0.5% of the TPC.
- Land purchase or lease costs and the preparation costs for the plant installation.
- Financing costs include the securing financing, fees and closing costs without considering the accrued interests during the plant construction which correspond to the 2.7% of the TPC
- Other owner costs, also known as lumped costs includes: preliminary feasibility study, economic development for incentivizing local collaboration and support, construction and/or improvement for transport infrastructure outside the plant site, legal fees, permitting costs, owner’s engineering staff for a third-party advice in EPC management, owner’s contingency related to delayed start-up or equipment cost fluctuation or unplanned labor incentives. The other owner’s costs account for the 15% of TPC.

In the end, the TOC estimate considering the various contributions is equal to 20.2 % of the TPC.

4.1.5 TASC estimation

As already mentioned, the TASC estimation accounts for the time effects during the capital expenditure period. In order to evaluate the escalation on investment capital during the construction period of the plant, two financial structures are introduced based on the type of developer/owner of the plant:

- The Investor-Owned Utility (IOU), in which the owner is also the main investor, is used for small plants as it allows the debt to be kept lower or at most equal to 50% of the investment and low interest reaching 9%

- The Independent Power Producer (IPP), in which the company that provides the majority of the capital is not also the owner of the plant, is used for large plants since the initial investment is higher as well as the debt that reaches 60% - 70% of the total investment. The interests applied in the IPP financial structure are also higher.

The NETL methodology provides several multiplicative and corrective factors in order to evaluate the TASC starting from TOC for the different financial structure, capital expenditure period and investment risk profile.

Finance structure	**High Risk IOU**		**Low Risk IOU**	
Capital expenditure period	Three years	Five years	Three years	Five years
TASC/TOC	1.078	1.140	1.075	1.134

Finance structure	**High Risk IPP**		**Low Risk IPP**	
Capital expenditure period	Three years	Five years	Three years	Five years
TASC/TOC	1.114	1.211	1.107	1.196

Table 31. Multiplying factors to obtain TASC from TOC **(12)**.

The CaL-CSP integration plant in question is owned by a group of companies that carry out research and development in the technological field and since it also provides investment capital, the IOU financial structure was chosen for the TASC estimation. The capital expenditure period is selected on the basis of the typical duration of a research project, i.e. three years. Furthermore, as preliminary project studies fully analysed the whole process in order to reduce the risk associated with recent technologies, a low risk scenario is considered.

Such considerations lead to the identification of the multiplication factor for the transition from TOC to TASC equal to 1.075 for each configuration of the heat exchanger network analyzed.

4.2 Discounted Cash Flow method

The effects of time on the investment capital are investigated using the Discounted Cash Flow (DCF) method proposed by the NETL Power Systems Financial Model with the aim of calculating the Levelized Cost of Electricity (LCOE), i.e. the cost of electricity

generation for a production system over its lifetime including the amortization of the initial financial capital.

4.2.1 WACC estimation

The DCF analysis required the calculation of the Weighted Average Cost of Capital (*WACC*) which represents the average cost of capital that the company pays to all its investors, shareholders and creditors based on the financial structure chosen for the investment. The *WACC* is defined as follows:

$$WACC = k_e \cdot \frac{E}{D+E} + k_d \cdot \frac{D}{D+E}$$

where *D* and *E* are the percentage of debt and equity according to the financial structure of the investment equal to $D = 50\%$ and $E = 50\%$, while k_e and k_d are the cost of equity and debt respectively.

The cost of equity k_e is assessed by considering two contributions:

$$k_e = R_f + premium$$

where:

- R_f is the systemic risk based on the evolution of the economic sector which usually corresponds to short-term government bonds, since it is the investment with the lowest risk. In the present case, the systemic risk is set equal to 1.046%, i.e. the value of the 10-year Italian BTP **(18)**
- The *premium* expected by the investors, that represent the specific risk of the investment, is calculated as:

$$premium = R_s + \beta \cdot (R_m - R_f)$$

  - R_s is the small stack premium due to the reduced liquidity for small investors, then for this case is $R_s = 0$
  - β is the correction factor for the specific investment and it is considered equal to 1
  - The difference between the market return and systemic risks $(R_s - R_f)$ is also defined as the Equity Market Risk Premium (EMRP) which represents the average interest obtained by investing in the market. The EMRP is set equal to 5.5% **(19)**

The cost of debt k_d is evaluated by considering two contributions:

$$k_d = IRS + spread$$

where:

- *IRS* is the Interest Rate Swap and expresses the difference between the fixed and variable interest. It is set equal to 0.06% **(18)**
- The *spread* is the increase in the interest rate which depends on the investors ability to return the capital and it is equal to 1%.

The following table summarizes the results obtained on the basis of the previous considerations for the *WACC* calculation.

D	E	k_e	k_d	$WACC$
50%	50%	6.55%	1.06%	3.80%

Table 32. Results for WACC evaluation.

4.2.2 Fuel consumption calculation for heating stage

The heating stages present in the proposed configurations of heat exchanger networks are fed by the exhaust gases exiting a combustion chamber, which in turn is fed by the natural gas. In order to satisfy the heating requirements, it is necessary to calculate the fuel volumetric flow rate that must be introduced into the combustion chamber to obtain the desired heat flux.

Firstly, the outlet temperature of the flue gases is assumed equal to the temperature of adiabatic flame T_{ad}, which in the case of natural gas only formed by CH_4 is 1963°C (20). After that, the specific heat that corresponds to the outlet temperature of the exhaust gases is determined using a calculation tool for the properties of the substances and is equal to 1364 $\frac{J}{kgK}$ (21). Once the flue gas outlet temperature and the specific heat have been assessed, the fuel mass flow rate is determined considering the number of heating stages and the maximum heat demand to be satisfied by means of the following formula:

$$\dot{m}_{f,g} = \frac{\emptyset_{heat\ demand}}{c_{p,f,g} \cdot (T_{ad} - T_{out})}$$

In order to determine the volumetric flow rate of the flue gases, it is necessary to evaluate the number of moles of CH_4 obtained through the stoichiometric combustion

reaction:

$$CH_4 + 2\left(O_2 + \frac{79}{21}N_2\right) \rightarrow CO_2 + 2H_2O + 2\frac{79}{21}N_2$$

The flue gases density are calculated both in normal and real conditions as follows:

$$\frac{kmol_{f,g}}{kmol_{CH_4}} = 1 + 2 + 2\frac{79}{21} = 10.52$$

$$\rho_{N,fg} = \frac{1 \cdot MW_{CO_2} + 2 \cdot MW_{H_2O} + 2\frac{79}{21} \cdot MW_{N_2}}{10.52\frac{kmol_{f,g}}{kmol_{CH_4}} \cdot 22.4\frac{Nm^3_{f,g}}{kmol_{f,g}}} = 1.23\frac{kg_{f,g}}{Nm^3_{f,g}}$$

$$\rho_{f,g} = \rho_{N,fg} \cdot \frac{293.15}{T_{ad}} = 0.162\frac{kg_{f,g}}{m^3_{f,g}}$$

The volumetric flow rate of the flue gases both in normal and real conditions can be evaluated as follows:

$$\dot{V}_{N,f,g} = \frac{\dot{m}_{f,g}}{\rho_{N,fg}}$$

$$\dot{V}_{f,g} = \frac{\dot{m}_{f,g}}{\rho_{f,g}}$$

Furthermore, to determine the fuel consumption it is necessary to derive the volumetric flow rate of CH_4 starting from its molar flow rate, as follows:

$$\dot{n}_{CH_4} = \frac{\dot{V}_{N,f,g}}{10.52\frac{kmol_{f,g}}{kmol_{CH_4}} \cdot 22.4\frac{Nm^3_{f,g}}{kmol_{f,g}}}$$

$$\dot{V}_{N,CH_4,stoich} = \dot{n}_{CH_4} \cdot 22.4\frac{Nm^3_{CH_4}}{kmol_{CH_4}}$$

As regards the volumetric flow rate of CH_4, in order to pass from normal conditions to real conditions, the ratio between normal and fuel temperatures must be considered, which in the present case are both equal to 20 °C:

$$\dot{V}_{CH_4,stoich} = \dot{V}_{N,CH_4,stoich}\frac{T_{CH_4}}{T_N} = \dot{V}_{N,CH_4,stoich}$$

The thermal losses associated with the combustion process are evaluated starting from the efficiency of a generic steam generator in the following way

$$\eta = 1 - P_I - P_D - P_C$$

where:

- P_I are the losses due to the unburnt reactants, which in this case is zero because the combustion reaction is stoichiometric
- P_D are the dispersion losses
- P_C are the "chimney" losses related to the residual thermal power lost in the exhaust gases; since the exhaust gases are not used for other purposes, the contribution of the losses to the chimney is considered null.

Therefore, the only significant contribution is related to thermal dispersion that can be assessed by consulting the regulations on heat generators (UNI TS 11300-2:2008) (22).

Once the thermal efficiency has been determined, the volumetric flow rate both in normal and real conditions are evaluated as follows:

$$\dot{V}_{N,CH_4} = \frac{\dot{V}_{N,CH_4,stoich}}{\eta}$$

$$\dot{V}_{CH_4} = \frac{\dot{V}_{CH_4,stoich}}{\eta}$$

The air volumetric flow rate is evaluated from the theoretical air used in the stoichiometric combustion reaction and the CH_4 volumetric flow rate as follows:

$$A_{th} = 2\left(1 + \frac{79}{21}\right) = 9.5\,\frac{Nm^3_{air}}{Nm^3_{fuel}}$$

$$\dot{V}_{N,air} = 9.5 \cdot \dot{V}_{N,CH_4}$$

$$\dot{V}_{air} = \dot{V}_{N,air}\,\frac{T_{CH_4}}{T_N} = \dot{V}_{N,air}$$

Finally, the combustion chamber volume can be assessed considering an averaged volumetric flow rates between the inlet gases and a residence time equal to 0.5 s:

$$\dot{V}_{ave} = \frac{\dot{V}_{CH_4} + \dot{V}_{air}}{2}$$

$$V_{comb,chamb} = \dot{V}_{ave} \cdot t_{res}$$

The fuel consumption and combustion chamber volume data are necessary to determine both the costs of the heaters and the costs related to their operation in order to calculate the *LCOE* for the heat exchanger network.

4.2.3 LCOE evaluation

The Levelized Cost of Electricity (*LCOE*) for the heat exchanger network is calculated from the evaluation of the annuity, i.e. the capital costs estimation for each component divided over the years of plant lifetime considering the monetary interest rate. The annuity is composed by two contributions: the first one is related to the capital expenditure and is calculated by means of the following formula:

$$Annuity_{CAPEX} = Y \cdot \frac{i \cdot (i+1)^n}{(i+1)^n - 1}$$

where:

- Y is the total capital cost which is assumed to be equal to the sum of the TASC of the components
- i is the interest rate of money considered equal to the *WACC*
- n is the lifetime of the plant equal to 25 years.

The second contribution accounts for the operational expenditure of the system, which in the case of heat exchanger network depends on the annual consumption of the natural gas used by the heaters. The OPEX annuity can be evaluated as follows (23):

$$Annuity_{OPEX} = C_{nat\ gas} \cdot \dot{V}_{CH_4} \cdot CF \cdot 8760 \frac{h}{year} \cdot 3600 \frac{s}{h}$$

where:

- $C_{nat\ gas}$ is cost of the natural gas expressed in $\left[\frac{\$}{m^3}\right]$
- $\dot{V}_{CH_4}$ is the methane volumetric flow rate for the combustion reaction $\left[\frac{m^3}{s}\right]$
- CF is the Capacity Factor that represents the ratio between the hours of system operation and the total hours in a year expressed in percentage. In particular, the CaL-CSP integration plant is expected to operate continuously throughout the year but interruptions due to any maintenance or operating difficulties must be considered, therefore the capacity factor is set equal to 80%.

The total Annuity $\left[\frac{\$}{year}\right]$ is calculated as expressed below:

$$Annuity = Annuity_{CAPEX} + Annuity_{OPEX}$$

Once the electrical power produced in one year by the plant has been evaluated, the *LCOE* $\left[\frac{\$}{MWh}\right]$ of the heat exchanger network can be determined as follows:

$$LCOE = \frac{Annuity}{MW_{el} \cdot 8760\ h \cdot CF}$$

4.3 Results

In order to assess whether the improvements from the thermal point of view of the optimized configuration of the heat exchanger network determine as many economic advantages, it is necessary to perform the economic analysis of all the studied configurations.

4.3.1 Size parameters of heat exchanger network for continuous process

The proposed configuration for continuous process includes the heat exchangers both of the calciner side and the carbonator side and the components are:

- Two solid-solid heat exchangers in calciner side and one in carbonator side
- Three gas-solid heat exchangers both in calciner side and carbonator side
- One gas-gas heat exchanger in the carbonator side
- One cooler and two heaters both in calciner side and carbonator side

Based on the NETL methodology mentioned in the previous section, the C_{BEC} of each heat exchanger can be determined by calculating the variables of the two polynomial functions adopted for the different types of components, i.e. the areas of the heat exchangers and the volume of the heaters.

Gas-Gas Heat Exchanger				
HEX	***Φ[MW]***	$\boldsymbol{U\left[\frac{W}{m^2K}\right]}$	$\boldsymbol{\Delta T_{ml}[K]}$	$\boldsymbol{A[m^2]}$
B (carbonator)	3,62	100	20	**1810**
C1 (calciner)	12,73	35	15	**24243**
C2 (carbonator)	0,80	35	15	**1531**

Table 33. Gas-gas heat exchangers features for continuous process.

The Global Heat Transfer Coefficient *U* for gas-solid heat exchangers is calculated considering the heat transfer from both the gas and the solid side rearranged in the following expression:

$$U_{gas-solid} = \left(\frac{1}{U_{gas}} + \frac{1}{U_{solid}}\right)^{-1}$$

where the value of U_{gas} are the same reported in the Table. 25, while the U_{solid}value has been taken from literature (24). The *U* for solid-solid heat exchanger is determined by assuming that the heat exchange is performed by two gas-solid heat exchangers

connected indirectly by a heat transfer fluid with good thermal properties. Then, the size parameter of the solid-solid heat exchanger can be evaluated as follows:

$$(\Delta T_{ml})_{gas-solid} = \frac{(\Delta T_{ml})_{solid-solid}}{2}$$

$$(A)_1 = \frac{\emptyset}{2 \cdot (\Delta T_{ml})_{gas-solid}} = (A)_2$$

Hence, to guarantee solid-solid heat exchange two exchangers with the same exchange area will be required. The results of *U* calculation are summarized in the table below.

$U_{gas}\left[\frac{W}{m^2K}\right]$	$U_{solid}\left[\frac{W}{m^2K}\right]$	$U_{gas-solid}\left[\frac{W}{m^2K}\right]$
100	413	80,51

The size parameters for gas-solid and solid-solid heat exchanger are shown in Table. 33.

Gas-Solid Heat Exchanger				
HEX	***Φ[MW]***	$\Delta T_{ml}[K]$	$UA\left[\frac{W}{K}\right]$	$A[m^2]$
2 (calciner)	18,36	20	918344	**11407**
3 (calciner)	4,29	114	37618	**467**
5 (calciner)	18,03	20	901416	**11197**
A (carbonator)	25,45	20	1272256	**15803**
C (carbonator)	32,91	20	1645674	**20441**
D (carbonator)	9,62	119	80635	**1002**

Table 34. Gas-solid heat exchangers features for continuous process.

Solid-Solid Heat Exchanger				
HEX	***Φ[MW]***	$\Delta T_{ml}[K]$	$UA\left[\frac{W}{K}\right]$	$A[m^2]$
1 (calciner)	95,11	10	9511110	**118140**
4 (calciner)	93,36	10	9335790	**115963**
E (carbonator)	29,60	10	2959808	**36765**

Table 35. Solid-solid heat exchangers features for continuous process.

Heaters	*Φ[MW]*	$V[m^3]$
H1 (calciner)	4,21	**3,53**
H2 (calciner)	5,43	**4,55**
H1 (carbonator)	34,76	**29,16**
H2 (carbonator)	1,32	**1,11**

Table 36. Heaters features for continuous process.

4.3.2 Size parameters of heat exchanger network for batch-process

The heat exchanger networks proposed in *Configuration 2* and *Configuration 3* show the most interesting results in terms of cost estimation, as they are the only viable solutions to operate in day and night mode. The following tables show the results for the size parameters of the system components of both configurations

Configuration 2					
Gas-Gas		***Gas-Solid***		***Solid-Solid***	
HEX	$A[m^2]$	***HEX***	$A[m^2]$	***HEX***	$A[m^2]$
H	372	**A**	19517	**B**	9874
L	8	**C**	6763	**F**	86019
C1	9882	**D**	6267		
		E	18052		
		G	8305		
		I	50		

Table 37. Size parameters of heat exchangers for the batch-process for Configuration 2.

Configuration 3					
Gas-Gas		***Gas-Solid***		***Solid-Solid***	
HEX	$A[m^2]$	***HEX***	$A[m^2]$	***HEX***	$A[m^2]$
F	1810	**A**	17268	**B**	17757
G	372	**C**	6763	**H**	43010
M	8	**D**	733		
C1	9883	**E**	15803		
		I	8305		
		L	50		

Table 38. Size parameters of heat exchangers for the batch-process for Configuration.

The heaters characteristics are the same for both configurations and shown in the table below.

Heaters		
Heaters	***Φ[MW]***	$V[m^3]$
H1	3,62	**3,04**
H2	3,12	**2,62**
H3	34,75	**29,15**
H4	2,18	**1,83**

Table 39. Size parameters of heaters for the batch-process for Configuration 2 and Configuration .

The main differences between the two configurations concern the heat exchange areas and the number of heat exchangers. In fact, *Configuration 2* has ten heat exchangers (excluding cooling devices and heaters) while *Configuration 3* has eleven. However, some exchange areas of *Configuration 3* are smaller than in *Configuration 2*. The operational advantage of *Configuration* 3 lies in the possibility of using the same exchangers both in day and night mode, avoiding the addition of other heat exchangers that allow operation during the discharge phase with only carbonator system streams as shown in the figure below.

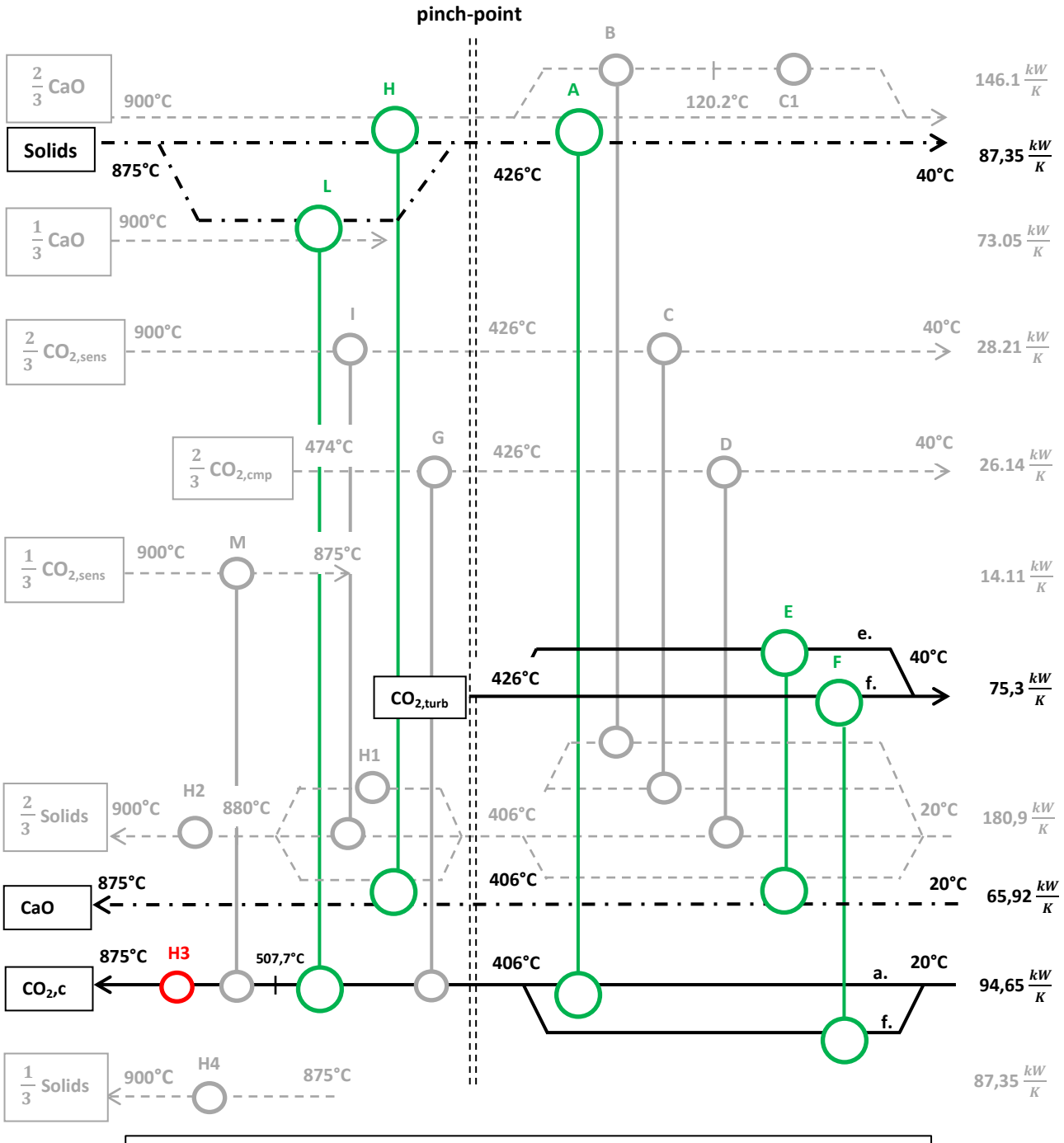

The configuration shown represents the night mode operations according to the considerations described in the previous section, maintaining the same network of heat exchangers as in *Configuration 3* which, however, operate with the carbonator system streams.

The gray dotted lines represent the streams that exist in the batch period of 8 daytime hours, just as the gray heat exchangers are active for the same time period. The black point-to-point lines represent the streams existing in the batch period of 16 night hours, i.e. the cold CaO stream extracted from the storage tank as it is no longer sent by the calcination system and the solid $CaCO_3$+CaO stream that leaving the carbonator since it is no longer sent directly to the solar calciner. Finally, the black lines represent the streams that exist continuously throughout the 24 hour batch cycle, i.e. the CO_2 flow leaving the gas turbine and the one entering the carbonator.

4.3.3 Cost estimation results

Once the feasibility of the configuration of the batch process for the charging and discharging phase of the CaL-CSP integration plant was verified, the cost analysis established that the plant improvements also lead to economic benefits. The following tables show the results of the cost estimation of the heat exchanger network for both the continuous and the batch processes.

Component	**Continuous process**	**Batch-process**
	$C_{BEC,2018}$[$]	$C_{BEC,2018}$[$]
Gas-gas HEX	$ 5.604.043	$ 3.497.444
Gas-solid HEX	$ 471.496	$ 380.349
Solid-solid HEX	$ 1.582.859	$ 849.776
Heaters	$ 690.993	$ 668.725
Total	**$ 8.349.392**	**$ 5.396.294**

	TASC [$]	**TASC [$]**
Total	**$ 22.670.606**	**$ 14.652.237**

Table 40. Cost estimation of the heat exchanger configuration for the continuous and batch processes

As can be seen from the results obtained, the capital expenditure of the batch-process configuration are reduced by approximately 35% with respect to the continuous process consequently to the reduction of the heat exchange areas.

4.3.4 LCOE results

By means of the Discounted Cash Flow method, the *LCOE* can be assessed starting from the calculation of the *Annuity* as reported in the previous section. The results for continuous and batch processes are summarized in the following tables.

Component	Continuous process	Batch-process
Annuity, CAPEX $\left[\frac{\$}{year}\right]$	1.421.130	918.491
Annuity, OPEX $\left[\frac{\$}{year}\right]$	5.415.403	4.483.286
Total $\left[\frac{\$}{year}\right]$	**6.836.533**	**5.401.776**

	LCOE $\left[\frac{\$}{MWh}\right]$	***LCOE*** $\left[\frac{\$}{MWh}\right]$
Total	**170,14**	**138,73**

Table 41. Discounted Cash Flow analysis for the continuous and batch process.

The capital expenditure annuity has been estimated considering the TASC obtained in the cost estimation analysis. Since the heat exchangers and the coolers do not use any resources for their operation, the annuity for operating expenditure counts only the contribution of the heaters and is determined assuming the cost of fuel equal to 0,372 $\left[\frac{\$}{year}\right]$ and the fuel consumption of each heat exchanger.

In the end, the *LCOE* for continuous and batch processes is assessed on the basis of the net electrical power produced by system: for the direct configuration of the CaL-CSP integration plant the electrical power of the gas turbine is equal to 37,3 MW_e from which the electrical powers used by the compressors and the solids transport system must be subtracted. Then, the Net Gross Electricity of the CaL-CSP integration plant is equal to 542 MWh.

Conclusions

In the first part of this work, the main characteristics of the Calcium Looping process were introduced in order to evaluate its application in the field of thermochemical storage system integrated with CSP technology as studied in the SOCRATCES project. The essential components of the CaL-CSP integration system used in the various proposed plant configurations were presented. Furthermore, the direct and indirect configurations analyzed in the SOCRATCES project were illustrated, but the direct configuration of the system with a CO_2 closed cycle was chosen for this treatment. The mass and energy balance equations of the CaL-CSP process have been defined in order to examine the main characteristics of the currents that take part in the process (CaO, CO_2 and $CaCO_3$) and to define the mass flow rates that guarantee correct operation during the charging and discharging phase of the storage system.

Being a production process in which rather high temperatures are reached (the inversion temperature of the carbonation /calcination reaction is equal to 900 ° C), the possibility of performing heat recovery among the process streams has been assumed. Pinch-analysis was used to design a heat exchangers network considering the CaL-CSP process as continuous, i.e. time independent. The first configuration proposed is able to keep the charging and discharging phase of the CaL-CSP process independent providing a network of heat exchangers for the carbonator side and one for the calciner side. However, the charging and discharging process of the CaL-CSP integration system is time-dependent, as the operation of the solar calciner is closely linked to the presence of solar radiation. Therefore, the pinch-analysis methodology for batch processes was introduced to evaluate any improvements in the design of the heat exchanger network that would allow the plant to operate continuously, despite the intermittence of solar thermal production applications. After analyzing various configurations, an optimized heat exchangers network for batch process capable of operating in the charging and discharging phase of the storage system was obtained. Finally, through economic analysis it has been shown that the configuration obtained for the batch process leads to economic savings compared to the configuration of the continuous process.

References

1. SOCRATCES project. [Online] https://socratces.eu/the-project/.

2. **P. Pardo, A.Deydier, Z.Anxionnaz-Minvielle.** A review on high temperature thermochemical heat energy storage. *Renewable and Sustainable Energy Reviews.* February 2014, pp. 591 - 610.

3. **Alovisio.** Process Integration of a Thermochemical Energy Storage System Based on Calcium Ooping Incorporating Air/CO2 Cycles in CSP Power Plant. July 2015.

4. **Tesio.** Power generation alternartives or small scale concentrated solar power plants with energy storage based on Calcium-Looping. 2018.

5. **C. Ortiz, J.M. Valverde, R. Chacartegui.** The Calcium-Looping (CaCO3/CaO) process for thermochemical energy storage in Concentrating Solar Power plants. *Renewable and Sustainable Energy Reviews.* 2019, 113.

6. **R. Chacartegui, A. Alovisio, C. Ortiz.** Thermochemical energy storage of concentrated solar powerby integration of the calcium looping process and CO2 power cycle. *Applied Energy.* 2016, Vol. 173, pp. 589-605.

7. *Optimizing the CSP-Calcium Looping Integration for Thermochemical Enegy Storage.* **A. Alovisio, R. Chacartegui, C. Ortiz.** 2017, Enery Conversion Management, pp. 85-98.

8. **T. Hills, P. Lisbona.** *SOlar Calcium-looping integRAtion for Thermo-Chemical Energy Storage. Solar calciner design.* s.l. : Research and Innovation Action (RIA), 2018.

9. **Guelpa E., Tesio U., Verda V.** *SOlar Calcium-looping integRAtion for Thermo-Chemical Energy Storage. Power cycles: scheme,models, analysis.* s.l. : Research and Innovation Action (RIA), 2019.

10. **V.Verda, E. Guelpa.** *Metodi termodinamici per l'uso efficiente delle riorse energetiche.* s.l. : Società Editrice Esculapio, 2013.

11. **Kemp, I.** *Pinch-Analysis and Process Integration.* s.l. : Elsevier, 2006.

12. **J. Wimer, W. Summers.** *Quality Guideline for Energy System Studies: Cost Estimation Methodology for NETL Assessments of Power Plant Performance.* s.l. : DOE/NETL, 2011.

13. *Appendix A. Cost Equations and Curves for the CAPCOST Program.* **D. Bhattacharyya, J. Shaeiwitz, W. Whiting, R. Bailie e R. Turton.** s.l. : Prentice Hall,, 2012, Vols. pp. 909-940.

14. **M. Marchionni, G. Bianchi, M. Konstantinos e A. Savvas.** Techno-economic comparison of different cycle architectures for high temperature waste heat to power conversion systems using CO2 in supercritical phase. *Energy Procedia.* 2017, Vol. 123, pp. 305-312.

15. **H. P. Corporation.** *The Basics of AIR-COOLED HEAT EXCHANGERS.*

16. **K. Albrecht e C. Ho.** Design and operating considerations for a shell-and-plate, moving packed-bed, particle-to-sCO2 heat exchanger. *Solar Energy.* 2019, Vol. 178, pp. 331-340.

17. Chemical Engineering,. *https://www.chemengonline.com/2019-cepci-updates-january-prelim-and-december-2018-final/.* [Online] 2018.

18. Il Sole 24 Ore. *https://mercati.ilsole24ore.com/obbligazioni/spread/GBITL10J.MTS.* [Online] 2019.

19. KPMG. *https://assets.kpmg/content/dam/kpmg/nl/pdf/2018/advisory/equity-market-risk-premium-july-2018.pdf.* [Online] 2018.

20. The Engineering Toolbox. *https://www.engineeringtoolbox.com/adiabatic-flame-temperature-d_996.html.* [Online]

21. Increase Performance. *http://www.increase-performance.com/calc-flue-gas-prop.html.* [Online]

22. My Green Buildings. *http://www.mygreenbuildings.org/2013/05/25/perdite-al-mantello-caldaia.html.* [Online]

23. ARERA - Autorità di Regolazione per Energia Reti e Ambiente. *https://www.arera.it/it/dati/gpcfr2.htm.* [Online]

24. **Bisognina P.C., Schramm J.C.** Influence of different parameters on the tube-to-bed heat transfer coefficient. *Chemical Engineering & Processing: Process Intensification.* 2019.

25. Enel. [Online] [Cited:] https://corporate.enel.it/it/storie/a/2019/01/utilizzo-energie-rinnovabili.

26. **WWF.** [Online] [Cited:] https://www.wwf.it/il_pianeta/cambiamenti_climatici/effetti_aumento_co2/.

27. Piattaforma delle Conoscenze. [Online] http://www.pdc.minambiente.it/.

28. **A.Frazica, A. Miliozzi.** Sistemi di accumulo termico. [Online] http://www.pdc.minambiente.it.

29. **M. Benitez, J.M. Valverde.** Multicycle activity of natual CaCO3 minerals for thermochemical energy storage in Concentrated Solar Power plants. *Solar Energy.* 2017, 153, pp. 188-199.

30.

31. Engineers Edge. *https://www.engineersedge.com/thermodynamics/overall_heat_transfer-table.htm.* [Online]

32. Tempco. *https://www.tempco.it/wp-content/uploads/2012/12/calcolo-scambiatori_tc.pdf.* [Online]